2017

Simulation Modeling and Optimization of the Performance of the Solar Water Heating System at the Southland Leisure Centre

Tiwana, Navjeet

UNIVERSITY OF CALGARY

Simulation Modeling and Optimization of the Performance of the Solar Water Heating System at the Southland Leisure Centre

by

Navjeet Singh Tiwana

A THESIS

SUBMITTED TO THE FACULTY OF GRADUATE STUDIES

IN PARTIAL FULFILMENT OF THE REQUIREMENTS FOR THE

DEGREE OF MASTER OF SCIENCE

GRADUATE PROGRAM IN MECHANICAL ENGINEERING

CALGARY, ALBERTA

APRIL, 2017

Abstract

The Co-Generation heating system at Southland Leisure Centre (SLC) uses solar energy and natural gas to provide the necessary hot water supply for the swimming pools. This is one of the largest solar heating systems in Alberta. The system was modeled using TRNSYS software and its components to represent the various parts of the solar heating system. Experimental data from a previous project was simulated and used to assess the accuracy of the modeling. After the model was set-up and validated, the software was used to simulate the current SLC heat management system. The model was also used to investigate several possible system improvements. A number of operational and maintenance concerns have been identified, including lack of verification of current quality of glycol, overheating of the water-glycol mixture and data loss from the SLC building management system. Recommendations to improve system performance, include changing the temperature setting for when the system turns 'on', increasing the amount of energy the system can store and turning on the make-up water feed at the ideal times. The SLC solar heating system was found to not be financially beneficial under current energy prices. Future projects should ensure constant heat demand to maximize productivity. Analysis of the solar heating system at SLC provides important information to help future projects become more competitive.

Acknowledgements

I would like to give my sincere thanks to my University of Calgary supervisor, Dr. David Wood for his help, guidance and understanding as I tried to complete my studies while continue to work full time. His support and suggestions for the research and the thesis have been vital. I would also like to thank Athaudage Nadeekangani for provide me with the data, on the bases on which this research was performed.

I am grateful to my loving parents, siblings and my partner for their unyielding support.

Table of Contents

List of Tables

List of Figures and Illustrations

List of Symbols and Abbreviations

Symbol	Definition
A_c	Collector array aperture or gross of the collector efficiency
A_{ht}	Surface area of heat transfer
C	Capacitance of the collector, including fluid
C_h	Capacity rate of fluid on the hot side calculated by using
C_b	Bond conductance
C_{min}	Minimum capacity rate
C_p	Specific heat of collector fluid
C_{ph}	Specific heat of fluid on the hot side
D	Tube outside diameter
DC_{Signal}	Control signal to direct flow
DHW5T	DWH5 tank temperature
D_i	Inner tube diameter
$f_{motorloss}$	Fraction of pump motor inefficiencies that contribute to a temperature rise in the fluid stream passing through the pump
F	Standard fin efficiency for straight fins with rectangular profile
F′	Collector fin efficiency factor
F_R	Overall collector heat removal efficiency factor
G_{sc}	Solar Constant
$\overline{H}_d$	Monthly average daily diffuse radiation on a horizontal surface
$\overline{H}_o$	Monthly average extraterrestrial radiation on a horizontal surface
h_{fi}	Heat transfer coefficient between the fluid and the tube wall
HX1MUT	Inlet make-up water temperature for HX-1
HXFlow	Flow measured on the make-up water side through HX-1
IAM	Incidence Angle Multiplier
$IAM_{\theta l}$	Longitudinal IAM at angle θ
$IAM_{\theta t}$	Transversal IAM at angle θ
I_T	Incident solar available energy per unit area
$\dot{m}$	Flowrate at use conditions
$\dot{m}_h$	Fluid mass flow rate on the hot size

M_{j}	Mass of the fluid inside a small portion of pipe segment referred to as j
$\bar{\mathrm{n}}$	Monthly average hours of bright sunlight per day
$\overline{\mathrm{N}}$	Monthly average day-length
$\dot{\mathrm{P}}_{\mathrm{rated}}$	Total rated power of the pump
$\dot{\mathrm{P}}_{\mathrm{shaft}}$	Shaft power used for the pumping process
$\dot{\mathrm{Q}}_{\mathrm{fluid}}$	Energy transferred from the pump motor to the working fluid
$\dot{\mathrm{Q}}_{\mathrm{T}}$	Total heat transfer across the heat exchanger
Q_{u}	Useful energy output of a collector
S	Solar radiation absorbed by a collector
t	Time
T	Temperature of the collector fluid at any point
T_{hi}	Hot side inlet temperature
T_{hi}	Hot size inlet temperature
T_{ho}	Temperatures of the hot side outlet temperature
T_{j}	Temperature of the fluid inside a small portion of pipe segment referred to as j
T_{Win}	Temperature of inner tube wall
T_{Wout}	Temperature of outer tube wall
T_{a}	Ambient temperature
$\mathrm{T}_{\mathrm{avg}}$	Average solar collector temperature
T_{ci}	Cold side inlet temperature
T_{in}	Inlet temperature of fluid to collector
T_{pm}	Mean temperature of the absorber plate
$\mathrm{U}_{\mathrm{L/T}}$	Temperature-dependent thermal loss coefficient of collector per unit area.
U_{L}	Overall heat transfer coefficient
$(UA)_{\mathrm{j}}$	Overall loss conductance a small portion of pipe segment referred to as j
W	Tube spacing

Greek Symbol	**Definition**
ε	Emissivity of inner tube
σ	Stefan-Boltzmann constant
β	Slope

γ	Surface azimuth angle
δ	Declination
η	Efficiency of the solar collector
θ	Angle of Incident
ϕ	Latitude
$(\tau\alpha)_n$	Product of cover transmittance and absorber absorbance at normal incidence
γ_s	Solar azimuth angle
ε_{HX}	Heat exchanger effectiveness
$\eta_{pumping}$	Pumping process efficiency
θ_z	Zenith angle

Abbreviation	**Definition**
CHW	Commercial Hot Water
DHW	Domestic Hot Water (Tank)
EPC	Energy Procurement Construction
ETC	Evacuated Tube Collector
GHG	Green House Gas
ISP	Indoor Swimming Pool
LHS	Left hand side
OSP	Outdoor Swimming Pool
PPM	Parts per million
PV	Photo voltaic
SLC	Southland Leisure Centre
VAH	Ventilation Air Heating

1 Introduction

1.1 Background

Solar energy has been an integral part of life on earth. It is believed the energy from the Sun and solar storms may have been the catalyst for life to start on earth (Fox, 2016). Most forms of energy we use, including fossil fuels, come directly or indirectly from the Sun. Fossil fuels, even though non-renewable, are derived from solar energy and stored in the earth millions of years ago.

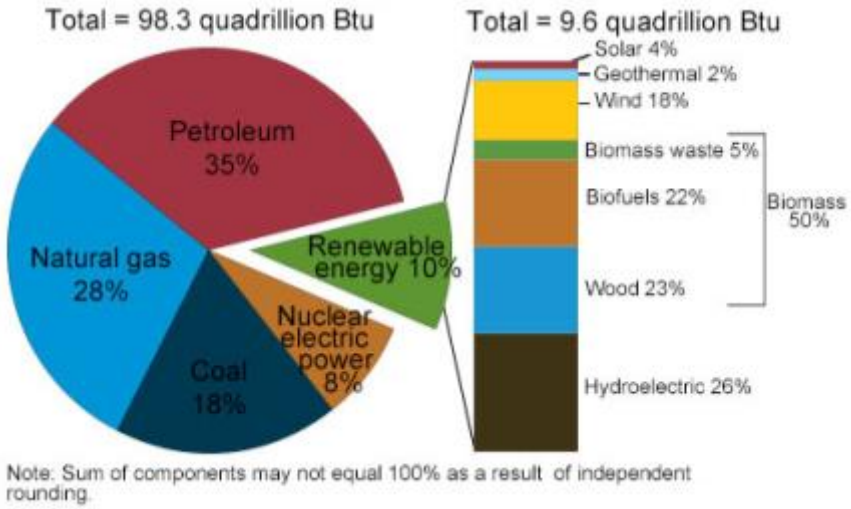

Figure 1: U.S. Energy Consumption by energy source in 2014 **(U.S. Energy Information Administration, 2015)**

As shown in Figure 1, 8% of the energy consumed in the U.S. was from nuclear electric power and geothermal energy was 0.2%. The remaining 92% come directly or indirectly from the Sun. (U.S. Energy Information Administration, 2015). Nuclear energy, even though abundantly available for current demand is considered non-renewable and has significant environmental impacts (U.S. Energy Information Administration, 2015).

Since 700 B.C. humans have used the Sun's rays through magnifying lenses to start fires (Department of Energy, 2004). Currently solar energy can either be harnessed directly in the form of solar thermal technology or as electricity produced by photovoltaic cells. During the year 1954 the first photovoltaic cells was able to achieve the efficiency of 4%. The Natural

Renewable Energy laboratory in the United States has been able to produces cells that are capable of achieving 30% efficiency in 1994 (Department of Energy, 2004). The highest efficiency acquired to date for PV cells was 46% in 2015 for a four-junction concentrator cell (NREL, 2017)

The research performed during the course of this report is based on solar thermal technology. Solar thermal energy collection converts energy from the sunlight into a form of heat energy that can be useful (Gill & Goldwater, 2007). Applications of Solar Thermal can include but are not limited to:

- Domestic hot water (DHW) heating
- Commercial hot water (CHW) heating
- Space heating of residences or buildings (ventilation air heating, or VAH)
- Heating an indoor swimming pool (ISP) or outdoor swimming pool (OSP)
- Agricultural uses such as water heating and crop drying (Gill & Goldwater, 2007)

There are a number of advantages of using solar energy over fossil fuels. The list of benefits are extensive but a few of the main advantages include:

- Solar energy has fewer carbon dioxide emissions: The increase in carbon dioxide in the atmosphere has raised the spectre of severe climate change. The parts per million (ppm) by volume of carbon dioxide in the atmosphere has risen from 280 ppm at the beginning of the industrial revolution, to 385 ppm in 2010 (Lackner, 2010)
- Solar energy is a renewable source of energy and will be available for billions of years (Damaschke, 2016)
- Solar energy systems usually require little maintenance when compared to conventional fossil fuel energy operations
- Solar modules (for PV) and panels (for solar thermal) do not produce noise and therefore can be placed in close proximity to residences
- Many governments are introducing incentives to companies / individuals to promote investment in solar or other clean energy systems (Damaschke, 2016)

- Generally speaking the electrical energy needed during the day peaks at the same time as does the supply of solar energy (in industrialized countries, a second peak in electricity demand can be in the evenings).

It is due to these advantages and concerns over climate change that the solar energy sector was growing at ten times faster than the American economy in 2013 (Sandry, 2013). This report is focused on the use of solar thermal heating in Calgary, Canada and more specifically the use of evacuated tube solar heaters for indoor pool heating, as described later in this report.

1.2 The Sun and Solar Radiation

The Sun is the direct and indirect source of most of the energy that is consumed by humans. The Sun mostly consists of hydrogen, some helium, and trace amounts of carbon, oxygen, nitrogen, and other heavier atom elements (Hathaway, 2010). The Sun is an intensely hot gaseous matter that has an overall diameter of 1.39×10^6 meters (Duffie & Beckman, 2013), which is more than 109 times the diameter of the earth. Due to the size and mass of the sun, the density at the core of the Sun is 10 times that of lead on earth (Hathaway, 2010). It is estimated that the inner temperatures of the Sun are in the range of 8×10^6 K to 40×10^6 K (Duffie & Beckman, 2013). The fusion reaction that occurs in the Sun when two hydrogen atoms fuse together to form a helium atom is the source of the energy that is radiated from the Sun.

Based on the energy that is released from the Sun and the distance of earth from the Sun there is a constant amount of energy that is available per square meter of the earth's surface. This value is based on the energy that would be received outside the atmosphere and is called the solar constant, G_{sc} (referred to as I_0 in Figure 2). Before the existence of rockets that could help take this measurement outside the atmosphere the solar constant had to be theoretically calculated; currently the World Radiation Center has adopted the valve of 1367 W/m^2 for G_{sc}.

Earth's distance from the Sun varies between 1.47 to 1.52 million kilometers throughout the year (Masters, 2003). This leads to the solar constant varying over the year as shown in Figure 2.

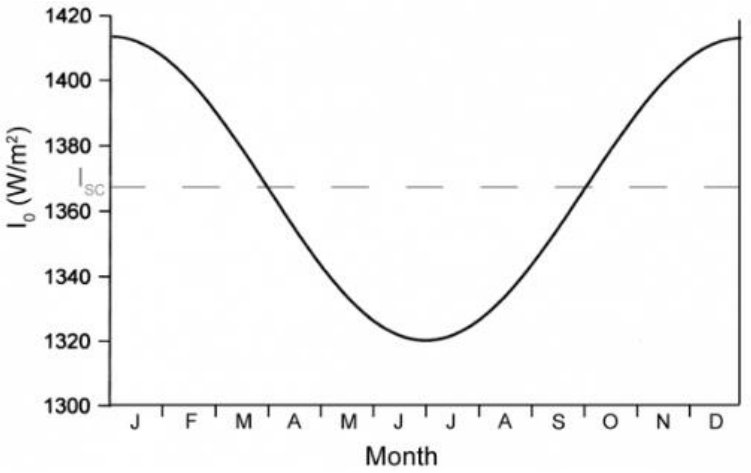

Figure 2: Variation of Solar Radiation with time of year **(ITACA, 2005)**

Where the solar constant is the amount of energy avaliable before the Sun's rays have passed through the atmosphere, it is the energy avaliable on the surface of the earth after the Sun's rays have passed through the atmosphere that is of relevence for terrestrial applications. As solar rays pass through the atmosphere their energy is reduced due to the presence of oxygen, ozone, carbon dioxide and water vapour (Hodge, 2010). In addition to the reduction in solar energy, some of the rays get scattered, changing their direction. **Beam radiation** is the radiation received from the Sun without having been scattered by the atmosphere (Duffie & Beckman, 2013). **Diffuse radiation** is the solar radiation received on the surface that has been scattered by the presence of the elements described above. On a clear day the the diffuse radiation can be as low as 10%, but on a cloudy day the diffuse radiation can essentially be 100% (Hodge, 2010). The avaliable total solar radiation energy is basically the sum of beam radiation energy and diffuse radiation energy.

There is also some radiation that is reflected from the earth's surface – this is called **reflected radiation**. Figure 3 shows the different forms of radiation that a tilted surface is subjected to.

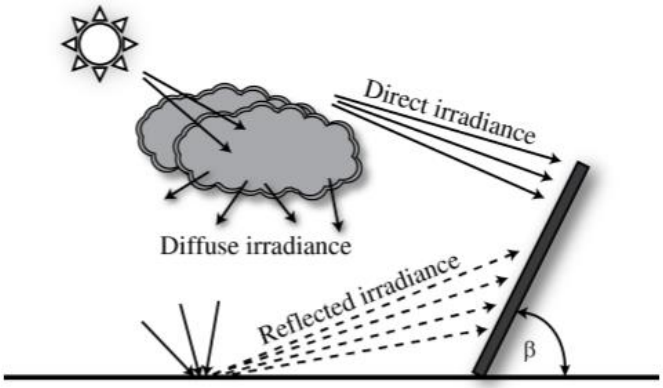

Figure 3: Different components of the solar radiation **(Gulin, Vaˇsak, & Baoti´, 2013)**

There are a number of geometric and regional factors that need to be considered when to determining the exact orientation of the surface in question to the Sun's rays and the earth's geometry.

θ **Angle of Incidence** is the angle between the Sun's rays and the normal to the surface in question.

θ_z **Zenith angle** is the angle between the Sun's rays and the vertical (Gulin, Vaˇsak, & Baoti´, 2013).

ϕ **Latitude** the angle of the location of interest when compared to the equator. North is defined relative to the equator and the range can vary from -90° to +90°, where the equator is zero.

δ **Declination** is the angular position of the Sun at solar noon with respect to the place of the equator. North is considered positive and the range can vary from -23.45° to +23.45° (Duffie & Beckman, 2013).

β **Slope** is the angle of the surface in question when compared to the horizontal. Figure 3 shows this angle with respect to a tilted surface. The slope angle range can vary from 0° to 180°.

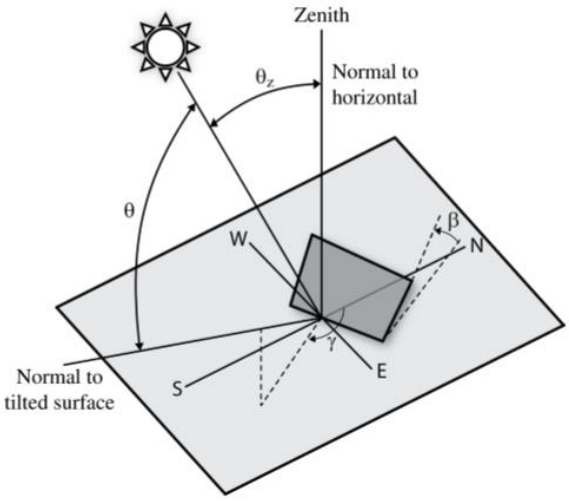

Figure 4: Zenith angle, angle of incidence, tilt angle (or slope) and azimuth angle on a surface **(Gulin, Vaˇsak, & Baotić, 2013)**

γ **Surface azimuth angle** is the deviation of the projection on a horizontal plate of the normal to the surface from the local meridian, with zero due south (Duffie & Beckman, 2013). East is considered negative and west is positive; the range can vary from -180° to +180°. Solar azimuth angle, γ_s is the angle on the horizontal plane between the Sun's rays and the south direction.

Based on all of these factors described above and a few other regional factors, the energy available to the solar collector can be determined.

1.3 Factors that affect the Solar Radiation at a given Location

The solar radiation that is available for harnessing at a surface is dependent on a number of factors. Considering that the studied system is in Canada the location plays a critical factor on the available energy that can be harvested. It should be remembered that these factors should be considered independently and even if one of the below conditions has a negative or positive effect on the solar radiation it can be overturned due to some other consideration. Below a number of these are discussed further.

1.3.1 Latitude

The latitude of the solar collector location plays one of the more significant roles on how much energy can be harvested. Because of this, there is an inherent disadvantage of harnessing solar

energy in Canada when compared to more tropical locations where the solar radiation is more abundant.

The further from the equator (north or south) the location is, the further overall available energy is reduced. This is because the incident angle (average throughout the year) to a horizontal surface increases with distance away from the equator and also the solar rays have to transverse through a longer length of the atmosphere. The longer distance travelled through the atmosphere cases more scattering and absorption of solar energy to the atmosphere. On the 21st of June at noon the Sun is at its highest angle in the northern hemisphere. It is directly overhead of the Tropic of Cancer; this is considered to the start of summer for the northern hemisphere and winter for the southern hemisphere. The opposite happens on December 21st with respect to the Tropic of Capricorn; this is when winter starts in the northern hemisphere and summer in the southern.

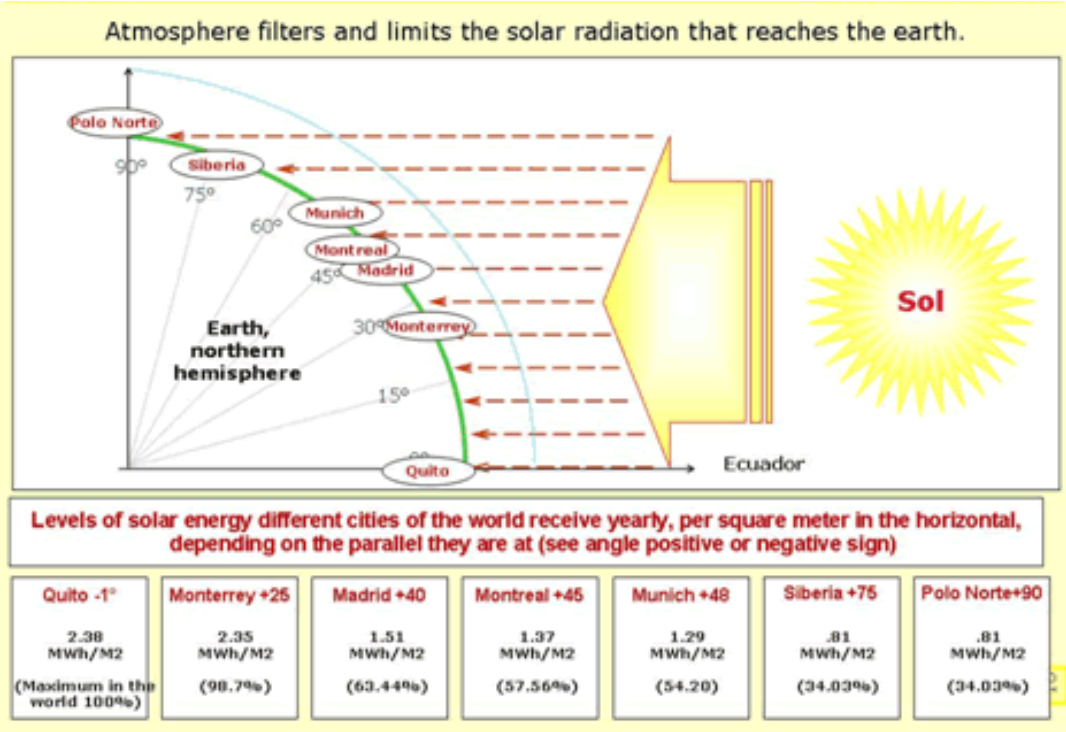

Figure 5: Amount of solar energy that is delivered in different parts of the world **(Gonzlez, 2005)**

Figure 5 shows the percentage of total energy that is available to harness based on a few different latitudes. Quito, Ecuador which is located just south of the equator has 2.38 MWh / m^2 of energy available on a horizontal plane. For a Canadian cities like Montreal, which is

located at ~45° latitude, this value is reduced to 1.37 MWh / m^2 (Gonzlez, 2005). For Western Canada, where the US border runs along the 49th parallel, the resource is further reduced. For the case of Calgary, where the latitude is 51°, this value can be interpolated to ~1.21 MWh / m^2, which is almost half of the energy available in Quito.

1.3.2 Shading and Clouds

Any physical obstruction to the Sun's rays can greatly affect the overall productivity of the solar energy system. Growth of plants and trees around solar energy systems must be controlled to avoid shading the system. Consideration should also be given to the potential shading of the solar collectors / reflectors by other solar collectors / reflectors in the system. This can be challenging for systems located in higher or lower latitudes where the solar altitude angle is usually low, leading to loss of system efficiency. Shading can be caused by supports too. Hottel and Woertz recommended that the theoretical radiation absorbed by the plate collector be reduced by 3% to account for shading effects if net unobstructed glass area is used for calculations (Duffie & Beckman, 2013).

Diffused radiation resulting from cloud cover can reduce the overall energy that is available to the solar system. The disadvantage of a higher latitude in Calgary can easily be offset by the lower number of clouds during the entire year. For solar heating, the importance of having good direct sunlight during the winter months when the requirement for heating is the highest is more important than during summer months when the heat demand is already low. Even though Vancouver is located in close proximity to the 49th parallel and Calgary is located in close proximity to the 51st parallel Vancouver receives an average of 1,938 hours of sunlight whereas Calgary receives an average of 2,396 hours of sunlight (Current Results Publishing Ltd, 2011). This is 24% more sunlight and the majority of the difference comes during the winter months when the heat demand is high.

1.3.3 Time and Date

The time of the day affects the amount of solar radiation energy. At night there is no solar energy available, whereas during the peak noon timeframe, when the Sun is at its highest, the largest amount of solar energy is available. Also, the amount of energy available in the summer

months is much higher than during the winter months. This is both due to the days being longer, allowing more time for energy harvesting, and also an increase in the intensity of the Sun's rays during the summer when compared to winter. Figure 6 shows the solar radiation measured by Natural Resources Canada, Calgary Station on a monthly basis.

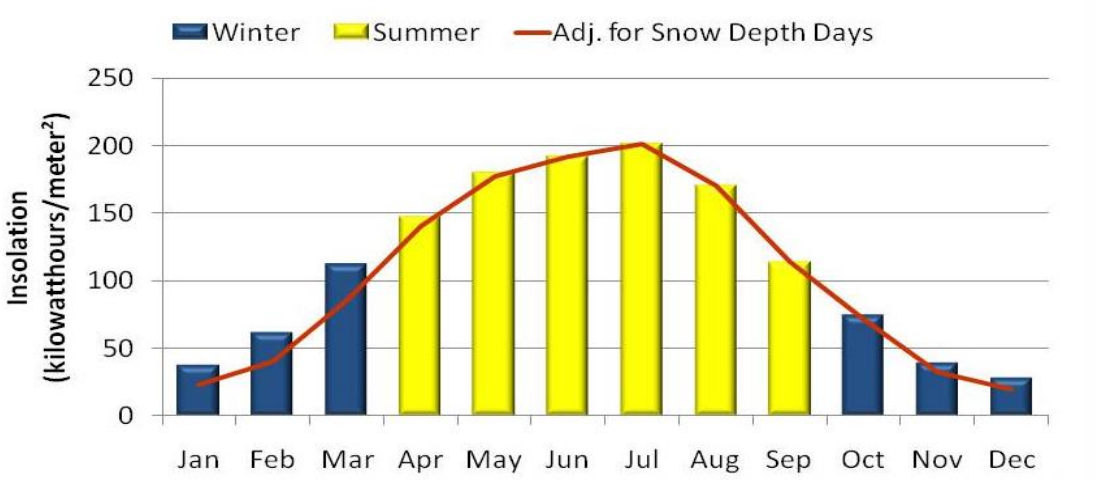

Figure 6: Solar Radiation by Month in Calgary **(Kitagawa, 2010)**

1.3.4 Dust and Snow

The effects of dust are difficult to quantify and generalize (Duffie & Beckman, 2013). Through experiments it has been found that if there is no rain (often the case in Calgary) and the climate is dry and dusty, then the overall reduction in absorbed radiation can be as high as 2% (Duffie & Beckman, 2013).

The effect of snow on a solar collector can be a very drastic reduction in the overall productivity of the system. Due to the high reflectance properties of snow it can take a long time for the snow to melt, until which the solar heat collector output would be reduced. When managing / operating solar collectors in low temperatures clearing of snow accumulation needs to be addressed immediately and frequently (Monto & Pillai, 2010).

1.4 Solar Collectors

A solar thermal collector is a device that is used to convert energy from solar radiation into heat. There are three forms of heat transfer in a solar thermal collector: conduction, convection and radiation.

Conduction is when heat is transferred from one molecule to another molecule in close proximity. In the case of a heat collector, conduction should be maximized between interconnected metal parts to maximize heat transfer to the desired working fluid, but minimized for heat losses. To reduce conduction losses the hot inner portion of a heat collector are thermally insulated from the exterior.

Convection is when heat is transferred from one medium to a working fluid that is heated and physically moved away from the heat source, thus taking the heat away. Forced convection results from pumping the fluid that is to be heated through a heat collector. To reduce convection losses there are envelopes that are installed over the hot inner portions of the heat collector (Duffie & Beckman, 2013).

Radiation is the transfer of heat in the form of electromagnetic waves. These waves can pass through space or through a transparent medium. The source of energy for a solar collector is radiation. There can be radiation losses from the system too and these need to be minimized.

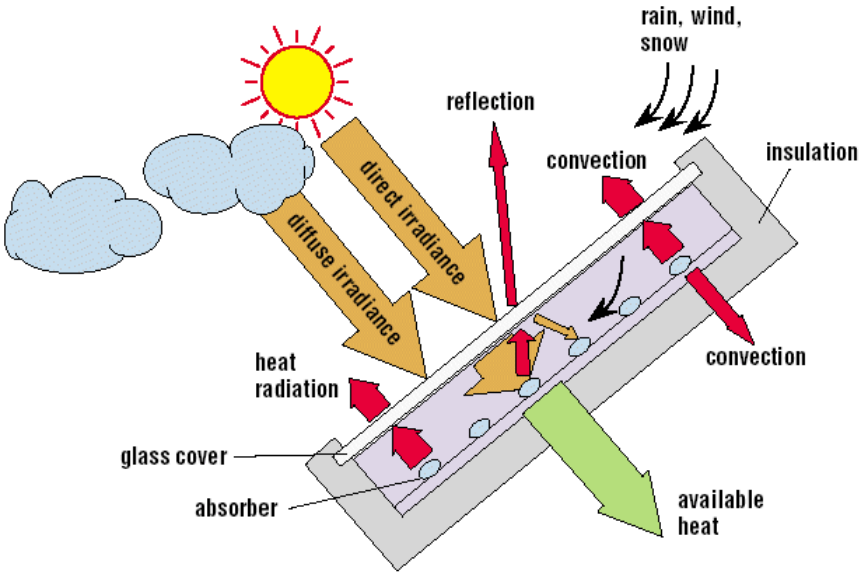

Figure 7: Illustration of different losses in a solar collector **(Quaschning, 2004)**

The overall goal of a well-designed solar collector is to maximize the solar radiation entering the system, maximize the heat transfer to the desired medium (water or other fluid) and minimize

the heat losses out of the system. Figure 7 shows the different forms of loses as described above.

1.4.1 Basic Flat Plate Collector

Flat plate collectors are the most commonly used solar thermal collectors currently in the market (Hodge, 2010). Basic flat plate solar panels can be designed to produce up to 100°C temperature difference between the ambient temperature and the heated fluid (Duffie & Beckman, 2013). The main components of a flat plate collector are a transparent front cover, an absorber and the insulated collector housing (Quaschning, 2004). Figure 7 shows the basic set up of a flat plate collector.

As the inner temperature of a flat plate collector can become very high (~200°C) when no fluid is being passed through it, the material used in the manufacturing of the flat plate needs to be able to withstand these temperatures without damage. A flat-plate collector usually consists of copper piping attached to a black absorber material inside of a glass-covered insulated frame (Gill & Goldwater, 2007). There are other variations of the materials that can be used, but the properties of the materials are consistent. The seals for a solar collector are essential as they stop dirt, humidity and insects from entering the collector and prevent heat from escaping the system.

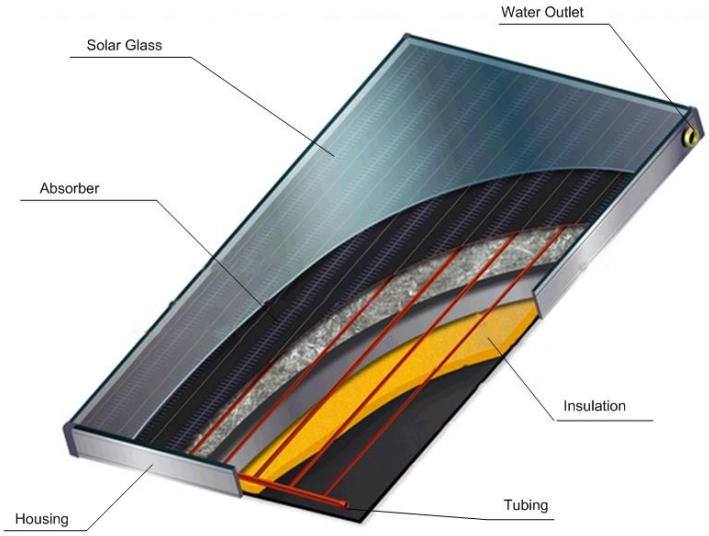

Figure 8: See through view of a basic flat plate collector **(Fred, 2010)**

Due to the difference between the ambient temperature and the temperature of the absorber there are convection and radiation loses. The convection is caused by air movement within the collector and by air passing over the glass cover; radiation losses exist between the absorber and Solar Glass and the Solar Glass and the environment (Quaschning, 2004). The glass cover helps reduce losses, but it also reflects some of the sunlight, preventing it from entering the heat collector.

Another method of reducing heat losses is to use selective coatings as absorbers that are efficient at absorbing energy, but once it has been absorbed only emit a small portion of the heat (Quaschning, 2004). This is achieved by using a substance that has a high absorbance of short wave radiation that comprise the Sun's rays and low emittance of long wave radiation (Duffie & Beckman, 2013).

1.4.2 Evacuated Tube Collector

While basic flat plate collectors work well for sunny warm climates their benefits are greatly reduced during cold, cloudy and windy days (Kalogirou, 2014). An improvement on the basic flat plate model is to reduce the convection losses due to the air movement inside the collector, this can be done by maintaining a vacuum between the cover and the absorber of the collector (Quaschning, 2004). This is very difficult to maintain in a flat plate collector as over time air makes its way into the collector through the seal between the cover and the housing (Quaschning, 2004). Other deficiencies of the basic flat pate collector include weather causing deterioration of internal material and the seals to fail, resulting in reduced performance of the solar collector (Kalogirou, 2014).

An evacuated tube flat plate collector generally has either a single or double closed glass tube under vacuum for insulation either throughout the system in the case of a single glass tube, or between the glass tubes in the case of a double glass tube (Gill & Goldwater, 2007). The basic principle of the evacuated tube collector (ETC) is similar to other solar collectors: an absorber located in the inner insulated tube converts solar radiation into heat. As the absorber heats up, it causes a fluid located in this region to evaporate, absorbing the energy. As this vapor rises, a small heat exchanger at the top of the tube absorbs the heat, causing the vapor to condense

and fall back down to the absorber region, thus allowing the process to repeat. The heat sink provides energy to the working fluid; the working fluid is usually being pumped through multiple collector's heat exchangers. Figure 9 shows the basic overall working of an ETC. It should be noted that the collector in the figure is shown horizontally, whereas in an actual installation, the heat exchanger is at the highest point.

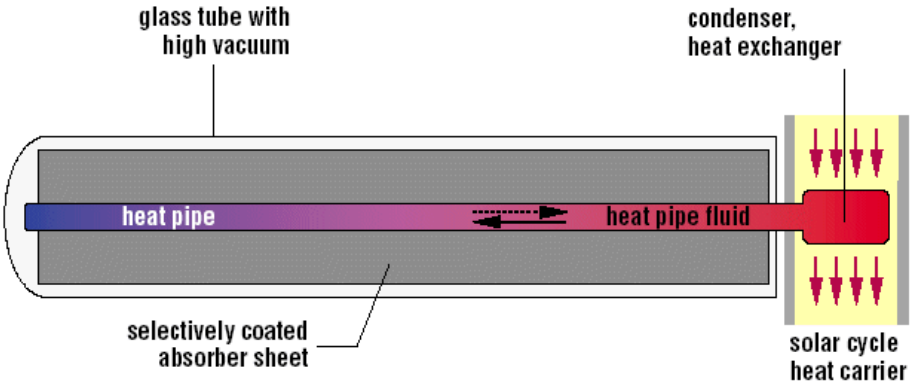

Figure 9: Working of a Evacuated Tube Collector **(Quaschning, 2004)**

The overall advantages of an ETC will be elaborated upon in later in this report, but generally speaking they include much higher operating temperatures, better insulation and are especially effective in colder climates (Kalogirou, 2014). One disadvantage of ETCs is the use of two working fluids. If the thermal system is to be used where temperatures fall below zero, a flat plate collector must use two fluids as well, so its natural advantage is lost.

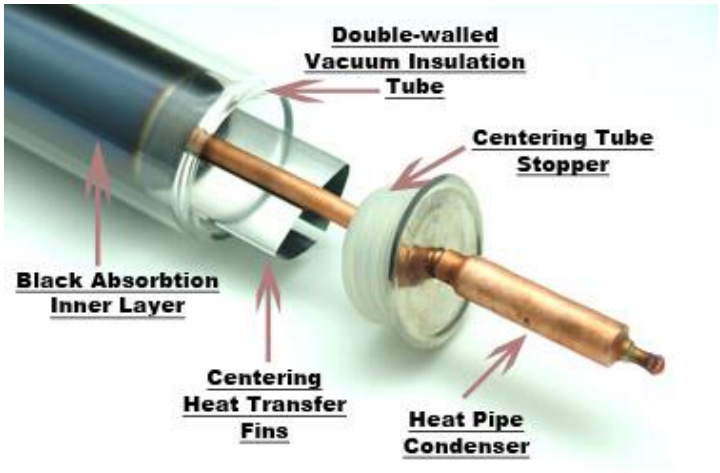

Figure 10: Open view of the Heat Pipe Evacuated Tube Collector **(Solar Pannels Plus, 2008)**

The ETC used at SLC is a heat pipe evacuated tube collector. It consists of a sealed copper pipe (heat pipe) bonded to a copper fin (absorber plate) that fills the evacuated glass tube. The working principles of a heat pipe collector are similar to what has been described above and Figure 10 shows cross section of a heat pipe collector. Note that to achieve good heating effect on a large volume of fluid a number of these tube collectors need to be used in series and parallel (Duffie & Beckman, 2013).

1.5 Solar Water Heating Systems

Domestic hot water heaters used in a typical house make up a good portion of the overall residential energy used in countries similar to Canada. The hot water can also be used for heating the interior of the house or solely for domestic hot water consumption. A solar water heating system usually has storage where hot water can be temporally stored while the demand of the hot water is low. When the demand for hot water rises, even if the Sun is not out, the stored hot water can then be used.

One of the most basic forms of a solar hot water system for small residential or small demand is to have the water storage at a higher elevation than the solar collectors, with pipe from the bottom of the water tank connected to the bottom of the collector (inlet to collector) and the top (outlet) of the solar collector connected to the top of the water tank. This is called the Thermosyphon system. This passive system works well as it does not need any pumping or active management system; the lower density of the heated water causes the water to flow to the tank and the cooler water takes its place through the water collector inlet (Gill & Goldwater, 2007). Though this system works well where the water tank can be stored above the collector, it is not always feasible for all types of roofs and houses and it also does not work well for larger systems or locations that have sub-freezing temperatures (Quaschning, 2004).

For cases where there is a high domestic hot water demand, multiple heat collectors can be used and pumps can be used for recirculating the fluid.

Swimming Pool

Instead of heating domestic hot water, the solar collector can also be used for other purposes like heating a swimming pool. Solar systems are favorable for heating swimming pools as generally speaking the temperature requirements are lower, therefore even on days when the system is not performing at its peak the solar system can still provide at least some of the heating load. There can be significant cost saving in using solar heating for swimming pools when compared to conventional means of heating (Gill & Goldwater, 2007).

Southland Leisure Centre (SLC)

The City of Calgary in collaboration with Enmax in 2011 started a project for solar thermal assisted heating at the Southland Leisure Centre (SLC) to reduce the natural gas footprint of the centre. There have been a total of 150 solar panels installed on the roof of the SLC to assist in the heating of the swimming pool and hot water used within the establishment. Each solar panel array includes 30 evacuated tube solar connectors. Figure 11 shows the type of panels installed at SLC. Williams Engineering Canada Inc. was the engineering firm that completed the overall design of the heating system at the SLC. The solar collectors face due south and this helps minimize shading.

Figure 11: The Solar collector used at SLC, model TZ58-1800-30R **(Kramer, 2007)**

The expectation was not to displace natural gas completely, but to reduce the overall consumption of natural gas by having solar energy assist in providing the heating load. As the external system is exposed to the cold winter climate in Calgary, water could not be used as the working fluid. Instead, a 50% mixture of water and glycol was used. This prevents freezing and bursting at temperatures as low as -36°C (ClenAir, 2013). At the SLC, the heat delivered from the working fluid loop is passed through heat exchangers and transferred to hot water. The heat is either stored for short term use in the Domestic Hot Water Tanks (DHW1 and DHW2) or used to heat the incoming water which is usually at temperature of 1-5°C during winter months (Nadeekangani, 2014).

During the summer months, protection is required to ensure the system does not overheat, causing damage to the working fluid, absorber and seals (Duffie & Beckman, 2013). In systems where glycol is used, the system needs to have over pressurization protection for events where the system overheats and the fluid boils (Gill & Goldwater, 2007). For SLC, if the fluid overheats the dry cooler can be used to exhaust heat to the environment. The system will be described in detail in Section 2.11.

1.6 Deliverables of the Report

Previous to this report, (Nadeekangani, 2014) measured the performance of a set of three panels of the SLC system. The intent of this report is to investigate the solar thermal system at the SLC at a macro level. This was performed from the foundation of the data that Nadeekangani (2014) had collected and to recommend any findings that might be if interest to the key stakeholders of this or future similar projects in Calgary or Canada.

The overall project deliverables of the report include:

1. Explain the theoretical formulas used for analysis of the solar data collected by (Nadeekangani, 2014)
2. Use the simulation software TRNSYS to model the SLC system and validate the model

3. Analyse the simulation data under the current building management system, identify any system components that are not functioning properly and provide feedback on operational concerns
4. Perform an economic analysis of the current operations of the SLC solar heating system and provide payback period
5. Based on the TRNSYS simulation runs, recommend system improvements, including changing the set-up for the solar heat collection system, changing the controller setting for when the system is to turn ‘on’ and documenting the expected gain from the recommended changes.

2 Literature Review: Solar collectors and Other Considerations

2.1 Introduction

As stated earlier, this study was performed to understand the workings of the solar heating system at the SLC at a macro level. Due to this, during the literature review, emphasis was given to the different concepts, factors and findings from previous studies. The heat balance and other equations used in the simulation were also covered during the literature review. In later chapters of this report, the understanding of how the simulation software is used should help with the understanding of the program.

The key interests addressed during the literature review include:

- How the measured data from the previous research can be used
- Theoretical understanding of the solar collector
- Considerations from literature that need to be included
- Considerations based on previous studies in similar geography and/or scope
- The theoretical basis and operation of the simulation software TRNSYS

2.2 Pyrheliometer and Pyranometer

As discussed in the introduction the solar radiation can be measured in the form of direct solar beam and indirect diffused radiation. A pyrheliometer is an instrument used to detect and measure the direct solar beam radiation solar radiation from the Sun and from a small portion of the sky around the Sun (Duffie & Beckman, 2013). Alternatively, a pyranometer is an instrument which measures the total hemispherical solar radiation (Duffie & Beckman, 2013). Total hemispherical radiation is the sum of the solar beam radiation and the diffused beam radiation. Figure 11 shows three pyranometers measuring total radiation at the right of the solar collector and one at the left measuring diffuse radiation by excluding the beam radiation with the help of a shading device. Figure 11 is taken from the report by the Fraunhofer Institute, Germany, on the performance test of the solar panels (Kramer, 2007). Commercial installations usually have at most one pyranometer for the whole system.

A CMP3-L model pyranometer was used by Nadeekangani (2014). A data logger was placed at the rear of the monitored panel on the roof of the SLC to record the measurements. The pyranometer has a working temperature range of -40°C to 80°C and can measure up to 2000 W/m^2 (Nadeekangani, 2014). The temperature range was within the range of temperatures typically seen in Calgary and the maximum radiation was not higher than 1100 W/m^2, which is usually the highest recorded value on the earth's surface (Duffie & Beckman, 2013). As already stated, the accuracy of the pyranometer used for the solar radiation measured over the period of a day is expected to have an accuracy of $\pm$ 10% (Nadeekangani, 2014).

Research performed by Iqbal (1979) for Montreal and Goose Bay, which have latitudes of 43° and 55° respectively, gave a formula that can be used for calculating the ratio between average diffused radiation and total radiation:

$$\frac{\overline{H}_d}{\overline{H}_o} = 0.163 + 0.478\left(\frac{\bar{n}}{\overline{N}}\right) - 0.655\left(\frac{\bar{n}}{\overline{N}}\right) \quad (1)$$

Equation (1) can be used to determine the ratio between $\overline{H}_d$, the diffused solar radiation available, and $\overline{H}_o$, the extraterrestrial radiation (Iqbal, 1979). Using 52% for $\bar{n}/\ \overline{N}$ (where $\bar{n}$ is the monthly average hours of bright sunlight per day and $\overline{N}$ is the monthly average day-length) for Calgary (Current Results Publishing Ltd, 2011) the percentage of diffused radiation for Calgary is calculated as only 7.1% of the extraterrestrial radiation.

2.3 Solar Collectors Basics

There are a number of factors that need to be considered when understanding the working of a solar collector. The efficiency of the solar collector is considered one of the essential factors. Before the efficiency can be introduced the overall useful energy needs to be explained. The steady state equation is

$$Q_u = S - A_c\left[U_L\ (T_{pm} - T_a)\right] \quad (2)$$

where, Q_u is the useful energy output of a collector, A_c is the area of collector, S is the solar radiation absorbed by a collector, U_L is the overall heat transfer coefficient, T_{pm} is the mean

temperature of the absorber plate and T_a is the ambient temperature . In the case of solar collectors under steady state, the useful energy is the difference between the absorbed solar radiation and the thermal losses as shown in Equation (2) (Duffie & Beckman, 2013).

$$\eta = \frac{Q_u}{I_T\, A_C} \tag{3}$$

where, η is the efficiency of the solar collector and I_T is the incident solar available energy per unit area. S in Equation (2) should be less than $I_T\, A_C$ in Equation (3) due to absorption and reflectance losses by the glass cover as explained in Section 2.5.3. Once the useful energy is known, the efficiency is simply the fraction of useful energy and the available energy as shown in Equation (3) (Duffie & Beckman, 2013).

With the maximum incident solar energy available of 1,100 W/m^2 (Duffie & Beckman, 2013), the yield of a solar collector system with multiple collector arrays can be significant. Though collectors can be used to heat an air medium directly, 99% of solar systems in Canada use a liquid medium (Gill & Goldwater, 2007). Although Equations (2) and (3) apply to any type of collector, ETCs have some differences when compared to flat plate collectors:

Performance: Flat plate solar collectors perform well in sunny warm conditions, but for cooler days the ETCs perform better. For ETCs, the vacuum insulation works well during winter months and is able to provide a much higher grade heat when compared to the flat plate collector (Gill & Goldwater, 2007).

Size and Weight: Flat plate collectors come in varying sizes and weights, but typically are 1.2m (4ft) by 2.4m (8ft) and weigh approx. 45 to 59kg (100 to 130lbs). For the case of the ETCs, the weight can range between 45 to 109kg (100 to 240lbs) (Gill & Goldwater, 2007) and a wide weight range exists as the ETC length can vary based on design / usage. Based on requirements panels can be made from different numbers of ETCs.

Cost: The cost of flat plate collectors is typically less than ETCs, but due to economy of scale in production and completion the cost of ETCs has been falling (Gill & Goldwater, 2007).

Maintenance: Even though flat plate collectors are built to withstand the elements, whenever there is a mechanical damage the entire flat plate collector needs to be replaced. In the case of ETCs, if there is any damage individual tubes can be replaced relatively easily and the system does not need to be shut down for the repair (Gill & Goldwater, 2007).

2.4 Evacuated Tube Collector Operation

The use of ETCs has increased in recent years. For cooler climates similar to Canada they have been very helpful in reducing greenhouse gas (GHG) emissions. There are a number of considerations given to the system when using evacuated tube solar collectors.

Taube and Carscallen (1985) found that if the evacuated tube solar collectors were covered by snow then the overall useful solar energy being harvested was reduced by ~90%. As de-mineralized water was used in the system it was found that they were successful in not having any scale buildup (Taube & Carscallen, 1985). The SLC does not use de-mineralized water for domestic use.

During previous research in Edmonton, it was found that all the leaks in the system over three years were minor. They were caused by poor design or workmanship and were not considered to be a systematic problem (Taube & Carscallen, 1985). It was also found that 2% of evacuated tubes lost their vacuum over a period of 28 months (Taube & Carscallen, 1985). Though that number is not too large, even the loss of a few tubes can reduce the efficiency of the system and cause losses in cooler climates. If rust inhibitors are used regularly in the system, then internal corrosion can be minimized and the system would not have corrosion problems during the system lifecycle (Duffie & Beckman, 2013).

Another consideration in the case of ETCs that use a water / glycol mixture is possible overheating. The system needs to be designed to ensure that the glycol mixture does not boil, as during boiling the solution becomes acidic and its properties deteriorate (Gill & Goldwater, 2007). This can be of concern as the ETCs have metallic parts that can be damaged by the acidic solution. Also overheating can cause the over-pressurization of the system. Considerations for

pressure relief valves and expansion tanks need to be captured in the design of these systems (Gill & Goldwater, 2007).

2.5 Energy Balance for Solar Heat Collectors

A more accurate and unsteady form of Equation (2) is

$$C\frac{dT}{dt} = F'\left(S - A_C\ U_L\ (T - T_a)\right) - \dot{m}\ C_p\ (T - T_{in}) \tag{4}$$

where, C is the capacitance of the collector (including fluid), t is the time, T is the representative temperature of the collector fluid, F' is the collector fin efficiency factor, T_{in} is the inlet temperature of fluid to collector, $\dot{m}$ is the flowrate at use conditions and C_p is the specific heat of collector fluid (Thermal Energy System Specialists, 2012). To be able to further expand on the setup of a heat collector Equation (2) can be used to derive the unsteady heat Equation (4) (Duffie & Beckman, 2013).

Equation (4) implies that the overall total energy change over a period of time at a given location on the collector is going to be equal to the total energy that is absorbed from the Sun minus the overall thermal losses and the change in internal energy of the system. The implication is true for any time interval, it can be used for both steady state and transient state. During the steady operation, the internal energy of the collector does not change over time as the left hand side (LHS) of Equation (4) is equal to zero.

2.5.1 Capacitance of a collector

The capacitance of a collector is the overall energy required to heat the collector by one unit of temperature. This includes heating the collector plates, tubing, fluid and any other component that heats up with the fluid. Capacitance can be important for collectors, as high values mean the system could take longer to heat up once the sun is out, but could keep working for a longer duration after the sun's rays are no longer available. Note that high capacitance can be a benefit in some cases and a drawback in others.

2.5.2 Collector fin efficiency factor

F' is the collector fin efficiency factor; the physical interpretation for F' in a physical location is the ratio of the actual useful energy gained to the useful energy that would have been gained had the overall collector surface been the same temperature of the local fluid temperature (Duffie & Beckman, 2013). F' is dependent on the geometry of the collector fin; the temperature gradient over the surface of the collector is factored into the collector heat equation with the help of the collector fin efficiency factor. Figure 12 shows the Temperature distribution on an absorber plate.

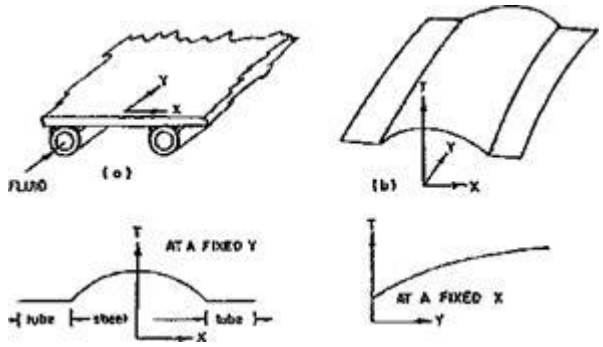

Figure 12: Typical temperature distributions on an absorber plate **(Duffie & Beckman, 2013)**

There are many factors that can affect the collector fin efficiency. When the distance between the tubes is reduced, material thickness or thermal conductivity is increased, and as expected, the collector fin efficiency factor increases. Duffie and Beckman state that F' is given by

$$F' = \frac{1}{U_L W \left[\frac{1}{U_L\,[D + (W - D)\,F]} + \frac{1}{C_b} + \frac{1}{\pi\, D_i\, h_{fi}}\right]} \tag{5}$$

where, W is the tube spacing, D is the tube outside diameter, F is the standard fin efficiency for straight fins with rectangular profile, C_b is the bond conductance, D_i is the inner tube diameter, and h_{fi} is the heat transfer coefficient between the fluid and the tube wall (Duffie & Beckman, 2013).

2.5.3 Incidence Angle Modifier

The Incidence Angle Modifier, IAM, is defined by

$$S = (\tau\alpha)_n \, IAM \;\; A_C \;\; I_T \tag{6}$$

where, $(\tau\alpha)_n$ is the product of cover transmittance and absorber absorbance at normal incidence. The radiation absorbed by the collector can be calculated using Equation (6) (Thermal Energy System Specialists, 2012).

The Incidence Angle Multiplier, is the ratio of the absorbed radiation at the current incidence angle to the absorbed radiation at normal incidence (Thermal Energy System Specialists, 2012). The geometry of the ETCs is optically not symmetric. The angle at which the Sun's rays make contact with the evacuated tubes determines the amount of solar radiation absorbed. Figure 13 shows the two different geometrical components the affect the IAM, θ_t and θ_l.

- θ_t, the transversal incidence angle and is the measurement of the angle between the Sun's rays and the normal to the collector plane along the transversal plane.
- θ_l, the longitudinal incidence angle and is the measurement of the angle between the Sun's rays and the normal to the collector plane along the longitudinal plane.

Both θ_t and θ_l have their own respective incidence angle multiplier factors that are represented by $IAM_{\theta t}$ and $IAM_{\theta l}$ respectively:

$$IAM_{\theta} = \; IAM_{\theta t} \;\; IAM_{\theta l} \tag{7}$$

Thus, IAM for any θ_t and θ_l can be approximated by multiplying $IAM_{\theta t}$ and $IAM_{\theta l}$ as discussed by (McIntire, 1982) and (Theunissen & Beckman, 1985), shown in Equation (7). The IAM values used for the solar collectors at SLC have been stated in Section 2.9.

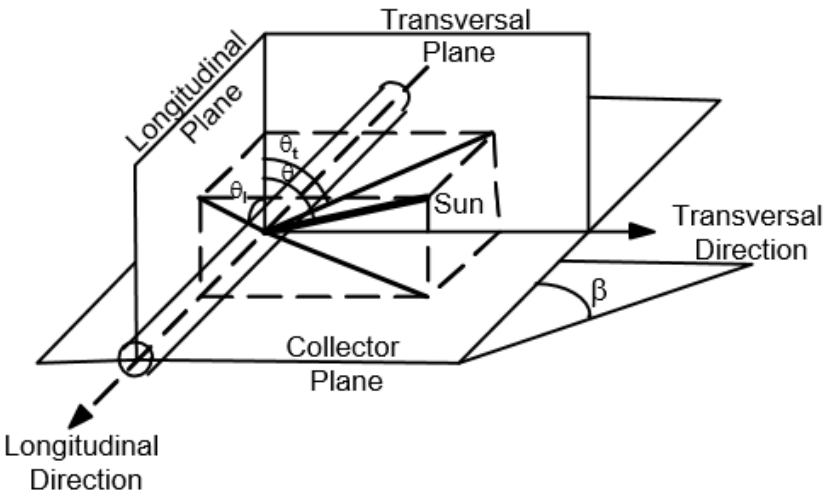

Figure 13: Longitudinal and Transversal Angles **(Thermal Energy System Specialists, 2012)**

2.5.4 Temperature dependent thermal loss coefficient

In Equation (4) the thermal loss was assumed to be linearly dependent on the difference between the ambient temperature and the fluid temperature at a given point. A more realistic relation for the thermal loss of the solar collector to the temperature difference between the fluid temperature and the ambient temperature is a quadratic relationship. This more accurate expression requires the addition of a term to Equation (4) with the new constant, $U_{L/T}$. Equation (8) shows the new relation where $U_{L/T}$ is the temperature-dependent thermal loss coefficient of the collector per unit area (Thermal Energy System Specialists, 2012).

$$C\frac{dT}{dt} = F'\left(S - A_c\ U_L\ (T - T_a) - A_c\ U_{L/T}\ (T - T_a)|(T - T_a)|\right) - \dot{m}\ C_p\ (T - T_{in}) \quad (8)$$

The equation is able to capture the variation of the thermal loss coefficient based on the change in temperature. Equation (8) can be used if the collector is divided into multiple small nodes and the calculation of say the temperature, T, can be performed multiple times. This is not a realistic approach when performing the calculation manually, but if a computer simulation software like TRNSYS is used then T is easily calculated. The collector can be evenly divided based on the number of nodes used; the exit temperature from one node can be treated as the inlet temperature for the consecutive node. As $U_{L/T}$ is a non-linear, if the fluid temperature changes, then using multiple nodes can increase the accuracy of the results.

2.5.5 Efficiency of Solar Collector

Similar to what was discussed in the previous section about the quadratic relation of the temperature difference, Equation (2) and Equation (3) can be modified to provide a more accurate efficiency relationship. Using Equation (8) for efficiency, the new efficiency formula is

$$\eta = F_R(\tau\alpha)_n - \ F_R\ U_L\ \frac{(T_i - T_a)}{I_T} - \ F_R\ U_{L/T}\ \frac{(T_i - T_a)|(T_i - T_a)|}{I_T} \quad (9)$$

(Thermal Energy System Specialists, 2012) Equation (9) can be simplified and re-written as

$$\eta = \eta_0 - \alpha_1 \frac{\Delta T}{I_T} - \alpha_2 \frac{\Delta T\ |\Delta T|}{I_T} \quad (10)$$

where, η_0, α_1 and α_2 constants for a given solar collector, (Kramer, 2007). The constant values used for the solar collectors at SLC are given in Section 2.9.

Equation (10) shows that as the final outlet temperature is increased the overall efficiency of the collector reduces dramatically. Also, when the fluid temperature is the same as the ambient temperature then there are no heat losses and the efficiency is equal to η_0. Thus, many solar thermal systems are designed through a trade-off between reducing the number of panels (increasing ΔT and reducing efficiency) and increasing the pump capacity to drive the working fluid around the system.

Ayompe and Duffy (2013) found that ETCs in Dublin, Ireland had an efficiency of 47% in December and 71% in May. Even with the relatively high efficiency of the tubes there were losses within the rest of the system and the overall system efficiency was 41% in December and 59% in May (Ayompe & Duffy, 2013). Overall efficiency, is defined as the ratio of the energy made available for use (after removing heat losses through piping and storage) to the solar energy projected on the solar collectors. These efficiencies are still satisfactory considering the climate and latitude of Dublin (~53° latitude). Even though the SLC has the same set temperature of 60°C for the heat storage tanks as the system studied by Ayompe and Duffy, the system set up and the heat storage demands are very different between domestic heating and a public indoor swimming pool.

2.6 Beam and Diffused radiation for Evacuated Tube Collector

The term S, solar radiation absorbed by the collector, can be divided into the different components introduced in Chapter 1. The total energy absorbed is the sum of the three components of the solar energy: the beam radiation energy, the diffused radiation energy and ground reflectance radiation energy. The overall transmittance-absorptance product of the collector is shown in

$$(\tau\alpha) = \frac{(\tau\alpha)_b \ I_{bT} + \ (\tau\alpha)_{ds} \ I_{dsT} + \ (\tau\alpha)_{dg} \ I_{dgT}}{I_T} \tag{11}$$

(Thermal Energy System Specialists, 2012) where $(\tau\alpha)_b$ is the $(\tau\alpha)$ for beam radiation, I_{bT} is the beam radiation incident on the solar collector, $(\tau\alpha)_{ds}$ is the $(\tau\alpha)$ for sky diffuse radiation, I_{dsT} is the sky diffuse radiation on the solar collector (tilted surface), $(\tau\alpha)_{dg}$ is the $(\tau\alpha)$for ground reflected radiation, and I_{dgT} is the ground-reflected diffuse radiation on the solar collector (tilted surface).

As stated, a pyranometer was used to measure that total radiation for the collector (Nadeekangani, 2014) and that data was used for this research. This way all three components of the available solar energy are considered. The incidence angle multiplier used during this research was verified by Kramer and also considers all three components of the solar radiation (Kramer, 2007).

2.7 Heat Losses for Evacuated Tube Collectors

The inside of the ETCs can achieve a much higher working temperature than flat plate collectors (Gill & Goldwater, 2007). The vacuum that exists between the inner tube and the outer tube is an excellent insulator to minimize heat losses. Conduction and convection losses can be significantly lowered or even completely eliminated with a good vacuum (Duffie & Beckman, 2013). However it is possible to have loss due to radiation given by

$$Inner\ Tube\ Heat\ Loss = \ \varepsilon \, A_{ht} \, \sigma \left({T_{Win}}^4 - \ {T_{Wout}}^4 \right) \tag{12}$$

where, ε is the emissivity of inner tube, A_{ht} is the surface area of heat transfer, σ is the Stefan-Boltzmann constant, T_{Win} is the temperature of inner tube wall, and T_{Wout} is the temperature of outer tube wall. Heat losses due to radiation can be calculated by using Equation (12) as stated by Zhao (Zhao, et al., 2009).

The radiation from the inner tube cannot pass through the borosilicate glass outer tube of a thickness greater than 1mm (Zhao, et al., 2009). Thus, P_t, the radiation energy losses transmitted through the outer glass, as shown in Figure 14 is equal to zero. A portion of the radiation is absorbed by the outer tube and a portion is reflected. The energy absorbed by the outer tube can be calculated by multiplying Equation (12) by α, the absorptivity fraction of the inner radiation to the outer tube (Zhao, et al., 2009). The inner tube heat loss can cause the external tube to heat up from radiation and that can cause convection losses to the surroundings from the external tube. Zhao found that with a good vacuum, these loss are small in nature even with the inner tube at 285°C and ambient temperature of 17.5°C, the outer tube temperature was 45.5°C (Zhao, et al., 2009).

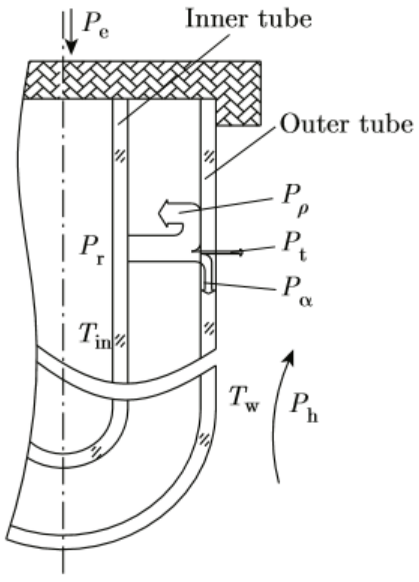

Figure 14: Schematic diagram of thermal balance of solar evacuated tube **(Zhao, et al., 2009)**

The losses from the outer tube are convective in nature. As the collectors are located on the exterior of the buildings the wind can cause forced convection and further increase the heat transfer coefficient and thus overall heat loss. A case study performed in New Delhi found the

wind speed along with the solar radiation, ambient temperature, heat losses from the absorber tube, angle of radiation incidence and tilt angle of collector are all contributing factors to the overall efficiency that can be achieved in an ETC (Kumar & Kumar, 2015). As there are various other factors in which the collector efficiency is dependent, and there are limitations of the components in the software that were used in this research, the wind speed that was measured by Nadeekangani at the SLC was not used in this research.

2.8 Temporary Solar Energy Storage

One of the disadvantage of solar energy when used for domestic space or water heating purposes is that the supply and demand usually do not coincide. To alleviate this problem there can be different ways that the solar heating system can be designed. In the case of the solar heated community Drake Landing, located in Okotoks, Alberta, the system stores heat over the summer months in a long term heat storage set-up underground and uses the stored heat in the winter months for domestic heating load, supplemented by gas powered boilers. Drake Landing is the first community in the world where over 90% of its residential space heating needs are met by solar thermal energy (Drake Landing Solar Community, 2005). Figure 15 shows the energy storage loop set-up that has been used in Drake Landing.

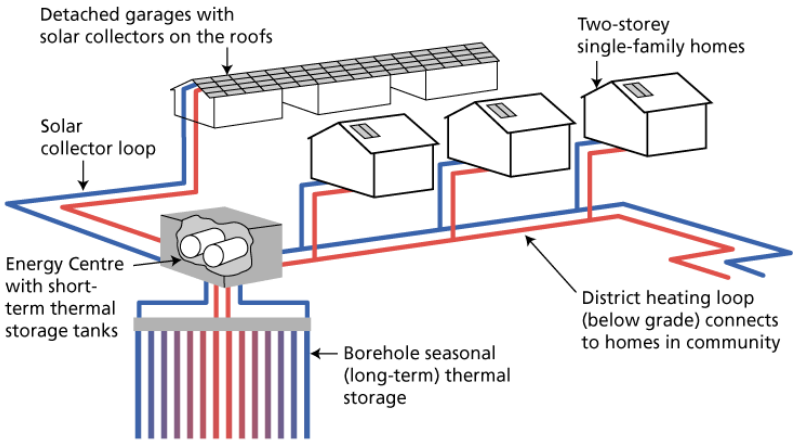

Figure 15: Collector / District Loop and Solar Seasonal Storage **(Drake Landing Solar Community, 2005)**

At the SLC, the heat load exists throughout the year, therefore long term heat storage is not needed. The SLC uses a heat exchanger and four water storage tanks where heat can be stored and used thereafter as needed for heating the swimming pool.

2.9 Evacuated Tube Collector Test Information

A test was performed by the Fraunhofer-Institute for Solar Energy Systems on the TZ58-1800 solar ETCs to validate the manufacturer's specifications. This is the same model of solar collector that has been used at the SLC. The specification of the collectors used at the SCL, TZ58-1800-30R, is shown in Table 1.

Table 1: Specification of the collectors used at SCL, TZ58-1800-30R **(Kramer, 2007)**

Brand name:	TZ58-1800-30R
Serial no.:	
Year of production:	2006
Number of test collectors:	1
Collector reference no. (ISE):	2 KT 57 001 102006 (function tests)
Total area:	2.025 m * 2.420 m = 4.901 m^2
Collector depth:	0.189 m
Aperture area:	1.710 m x 0.0544 m x 30 tubes = 2.791 m^2
Absorber area:	1.710 m x 0.0470 m x 30 tubes = 2.411 m^2
Weight empty:	106 kg
Volume of the fluid:	2,3 l (MS)

Testing standard EN 12975 found the zero loss efficiency for model TZ58-1800 to be 73.4% (Kramer, 2007). The constants for the solar collectors in Equation (10) for the TZ58-1800 series heat collectors can be found in Table 2.

Table 2: Efficiency constants for TZ58-1800 series heat collectors **(Kramer, 2007)**

η_0	0.734
α_1	1.529 W/m^2K
α_2	0.0166 W/m^2K^2

The Incidence Angle Modifier for the transversal and longitudinal angles was also confirmed by Kramer during the testing. With the help of Equation (7) and the data from Table 3 the IAM can be calculated.

Table 3: Measured (bold) and calculated IAM data for heat collector **(Kramer, 2007)**

θ:	0°	10°	20°	30°	40°	50°	53°	60°	70°	80°	90°
$K_{\theta T}$:	**1.00**	1.00	**1.03**	1.11	**1.25**	1.37	1.40	**1.36**	1.11	0.70	0.05
$K_{\theta L}$:	**1.00**	1.00	1.00	0.99	0.96	**0.92**	0.88	0.84	0.69	0.44	0.00

During testing the effective thermal capacity per square meter was found to be: 15.6 kJ/K m^2 (Kramer, 2007).

2.10 Solar Heating in Canada

Previously cited research from Ayompe and Duffy is the most applicable to the research at the SLC. There is very limited research that studies the effects of wind on the ETCs. There have been papers which state that the ETCs are the best source of solar thermal heating for a location like Alberta, Canada where winter temperatures can be as low as -40°C (Jackman, Lonseth, Lonseth, & Jagoda, 2009). There is no analysis presented in the paper to support this claim.

Other research found that up to 20% of Canadian residential energy load is domestic water heating (Islam, Fartaj, & Ting, 2004). Research has found that the current barriers to increasing solar market share include the cheap cost of natural gas and lack of public awareness of the costs and benefits of using solar heating for swimming pools (Islam, Fartaj, & Ting, 2004). Solar heating for swimming pools can have a payback period of 2 to 4 years and this has been confirmed by tests that have been performed at three different locations within Canada (Islam, Fartaj, & Ting, 2004).

2.11 Literature Specific to Southland Leisure Centre

During the research conducted at the SLC by Nadeekangani (2014) it was found that the outlet temperatures of one of the fifty different parallel flow set-ups exceeded the boiling temperature of the working fluid on a number of instances (Nadeekangani, 2014). The

equipment set up can be seen in Figure 16 below. Nadeekangani found that the flows was not consistent, the flowmeter showed negative flow rates even through the system uses a one-way flow valve. This is not how the system was designed to operate and could have been caused by the boiling of the 50% water / glycol mixture (Nadeekangani, 2014). During this research these findings were further examined to either verify if this is an overall system wide problem or a localized error within the array where Nadeekangani collected the data. The testing of the solar collector model used in the SLC was performed by the Fraunhofer-Institute for Solar Energy Systems (Kramer, 2007).

Figure 16: Location of where the Pyranometer was setup at SLC **(Nadeekangani, 2014)**

The collector efficiency calculated by Nadeekangani in the research for the valid flows / temperature ranged from less than zero to higher than 130°C. The consistent range on efficiency for the valid data was found to be between 20% and 80% (Nadeekangani, 2014), with no average value provided for summer or winter days. As shown by Ayompe and Duffy, it is expected that the system efficiency will be less than that of the collector due to additional losses. The solar data collected by Nadeekangani is the working basis for this research.

At SLC, the solar heating system is a closed loop. The harvesting of solar energy starts when the system flags that the solar collector temperature is high enough for adequate heat transfer to either the domestic storage tanks, or to the make-up water. The make-up water is the water supplied to SLC for domestic use and to compensate for water lost from the pool by evaporation. The source of the make-up water is the City of Calgary water distribution system.

In that case, the main pump turns on and starts the flow of the water-glycol mixture though the solar collector loop. The flow is then split to three different roofs at the SLC housing the solar collectors. A total of 150 solar collector panels are arranged in 50 parallel runs. The fluid goes through a set of three solar panels. There are flow limiting restrictions on all parallel runs, to make sure that the flow is regulated and all arrays have approximately the same flow. If the fluid temperature is too high, then the flow is directed to the dry cooler to cool the fluid down. Once back in the building, the fluid is directed to either the shell and tube heat exchanger, DWH5, that is used to temporarily store the energy, or to a flat plate heat exchanger that transfers the energy to the make-up water feed. The water from the DWH5 is further dispersed to the DWH1 and DWH2 tanks to increase the overall energy stored.

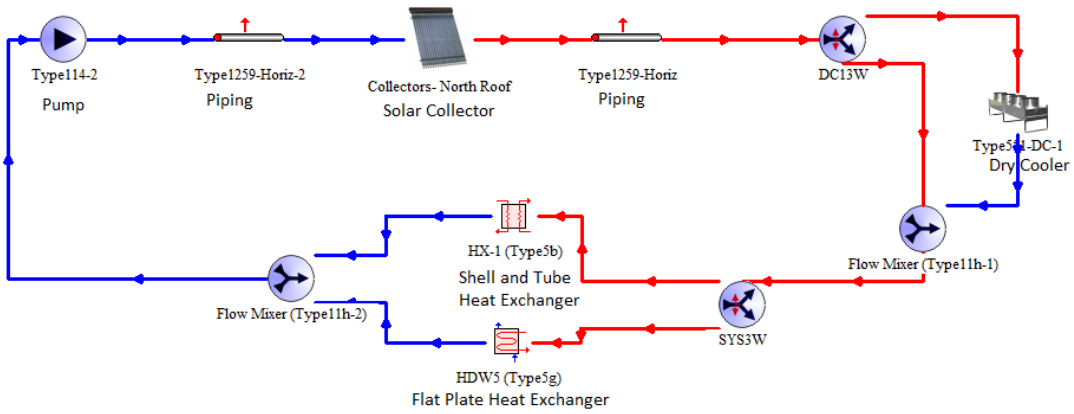

Figure 17: Basic system overview of SLC solar heating system

In order to optimize and validate the overall system performance, TRNSYS simulation software was used to run a simulation of the solar heating system at the Southland Leisure Centre.

3 Computer Simulation Software

3.1 Introduction to TRNSYS

TRNSYS is a graphics-based software that can be used to simulate a wide range of transient systems. Depending on the setup, TRNSYS can be used to simulate dynamic systems, including, but not limited to, thermal energy system, electrical energy systems, travel flow process or biological processes (Thermal Energy System Specialists, 2011).

The TRNSYS engine is the main processing component of the software. It reads and processes the input files and iteratively solves the heat balance and other equations. Through various iterations, the engine determines the convergence and plots the system variables (Thermal Energy System Specialists, 2011). The most critical part of any model in TRNSYS is the model set up and the different components used in the model. Similar to most modeling software, there is a trade-off between ease of implementation and flexibility of the model. There are more than 150 components that are available in the standard TRNSYS library and an additional 250 components available in fourteen different specialized libraries. The Standard Library and the Solar Collector Components library were used during this research.

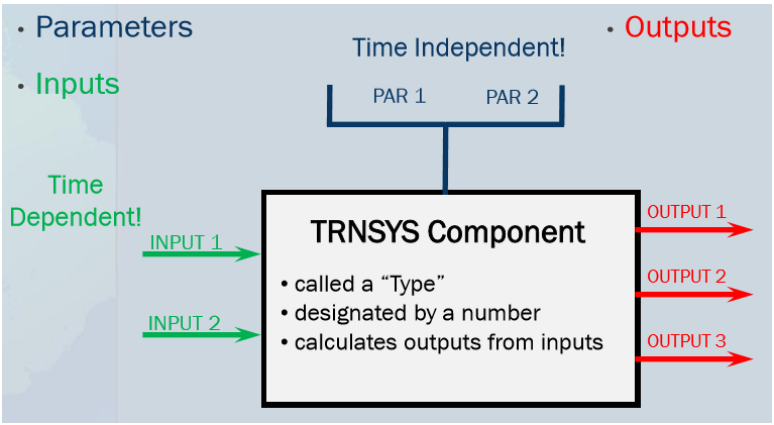

Figure 18: A component requires two kind of input information **(Duffy, Bradley, & Thornton, 2012)**

A component in TRNSYS is the building block of the model. The component itself has a working formula that is used to calculate the outputs based on the inputs and the component parameters. The parameters are fixed for a specific component and do not change over time;

however, the input can change over time. Figure 18 illustrates the inputs, outputs and parameters of a component.

For example, if a length of pipe was considered to be a component, the length, diameter, thickness and material property of the pipe could be the parameters of the pipe. The parameters do not change over time. The ambient temperature, fluid temperature, fluid flow rate and fluid specific heat when entering the pipe would be inputs of the component as they could change over the period of the simulation. When the simulation is run using the equations for the component, the inputs and the parameters, the software calculates the heat loss to the environment and the fluid outlet temperature over the simulation duration. The heat loss to the environment and the fluid outlet temperature can be considered the outputs of this component. Even through there are other simulation softwares available, the components available with TRNSYS make it an ideal software for solar thermal energy system similar to the SLC solar system. The equation used are stored within each component type and are set by the developers. To better understand the working of TRNSYS and how to use TRNSYS, the author attended a three day training session in Madison, WI organized by Thermal Energy System Specialists, the developers of TRNSYS.

The TRNSYS model can help, with the study and improvement of the system; as required, specific model inputs, or set parameters, can be changed and the end results can be compared. This is not feasible in the real world, as duplicating the solar radiation, duration of sun light, cloud cover, ambient temperature, inlet water temperature and demand of heat by the SLC is not feasible. Even if one was to consider just the duration sun light during the day, no two days in the year will have the same amount.

3.2 Simulation Driver and Outputs

As stated earlier, TRNSYS simulation solves through a re-iterative process. Similar to other components in the system, the driver for a simulation is also a component. The driver of the simulation provides information to other components on the bases of which the complete simulation is run. The outputs from the drives are the inputs that are used by other components within TRNSYS and outputs eventually lead to the simulation output. TRNSYS

needs the driver to have the data for the same time increments as the system set-up. The input data cannot always be easily entered and requires formatting to make sure it works as a correct TRNSYS input file. Examples of a simulation driver include the environmental information over the period of the simulation and data like solar radiation, wind speed etc. While setting up and validating a simulation, constant values or drivers that are theoretical can be used. Constant values can be a constant temperature, solar radiation, or any other values that can be used in the simulation to determine the steady state outputs. If these outputs are within the acceptable range to the recorded values during testing of the specific equipment, then the parameters used for the component can be considered validated. As the simulation is further refined, components can be replaced to make the model more accurate and realistic. When all constant values are used in a simulation, the results reach a steady state and will remain constant.

The non-physical components that are used to tabulate and record the results are considered outputs. The output can be plotted on a plotter component where it can be shown as graphs or extracted as a text file. The output data can be further processed through a number of components available in TRNSYS including the data integrator, graph plotter and other available components. A data integrator can be used to find the accumulated sum of a specific variable. For example, the data integrator can be used to integrate the total power used by a pump throughout the simulation. Figure 19 is a schematic showing the model drivers and outputs.

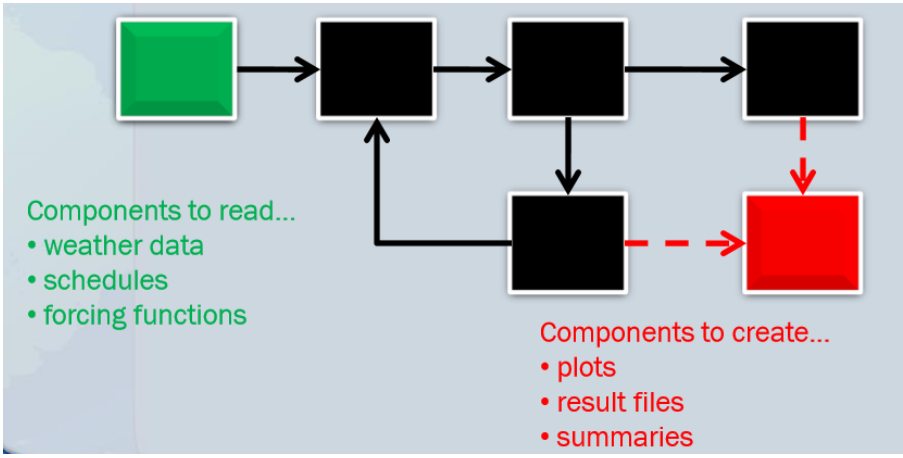

Figure 19: Green component is a driver and red component is an output **(Duffy, Bradley, & Thornton, 2012)**

3.3 Pipe Component

Although the components used in the TRNSYS model are explained in some detail in the following sections, the intent of these sections is to provide understanding of how these elements work. If further elaboration of the inner workings of the components is required the reader is referred to the TRNSYS component library (Thermal Energy System Specialists, 2012).

The pipe component, Type 31 is used in the SLC model to capture the heat loss to the environment when the working fluid travels between the indoor pump and the ETCs before being heated, and between the ETCs and heat exchanger. The component itself models the thermal characteristics of the fluid flowing through a pipe using variable size segments of the fluid. As more fluid enters the pipe, the existing fluid segments move further along. The size of the new mass segment is dependent on the flow rate and the simulation time step (Thermal Energy Systems Specialists, 2014). The outlet of the pipe are the segments that are pushed out due to the inlet flow. The limitation of this component is that the model does not consider the interactions and conduction between nearby segments. To avoid extensive calculations if there are too many segments in the pipe, adjacent segments are combined as one segment. The energy equation is

$$\mathrm{M}_j C_p \frac{dT_j}{dt} = -(UA)_j \left(T_j - T_a\right) \tag{13}$$

Equation (13) shows the differential equation that is used to solve for energy loss for each segment (Thermal Energy Systems Specialists, 2014). Here M_j is the mass of the fluid inside a small portion of pipe segment, $(UA)_j$ is the heat loss conductance of pipe segment j and T_j is the temperature of the fluid inside the segment j.

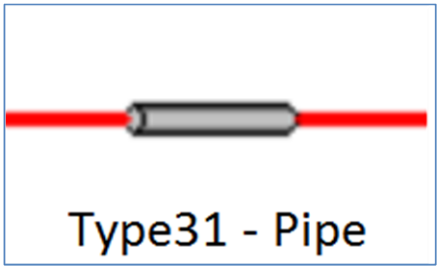

Figure 20: The icon used in TRNSYS to signify a pipe

3.4 Evacuated Tube Solar Collector Component

Type 538 component was used for the solar ETC in the model. The component is used as a collector in which the efficiency is based on the quadratic equation, Equation (10), with the values of the constants given in Table 2. The analysis of the solar radiation that is not perfectly normal to the collector surface is described in Section 2.5.3. The IAM values for different angles are input into the model through an external text file. As already stated, IAM can be calculated with the help of Equation (7) and the data from Table 3.

The solar arrays in this system can be set in a series under one component. This helps with the construction of the model, as otherwise there would be 50 different solar collector components modeled in each series. The capacitance of the array is also considered in the model and the values provided by the Fraunhofer-Institute for Solar Energy Systems (Kramer, 2007), outlined in Section 2.9 were utilized. Based on the provided parameters and inputs, the model calculates the collector fin efficiency, transmittance-absorptance product at normal incidence and the collector loss coefficient (Thermal Energy System Specialists, 2012). The solar radiation that is not normal to the collector surface is accounted for with the help of the IAM.

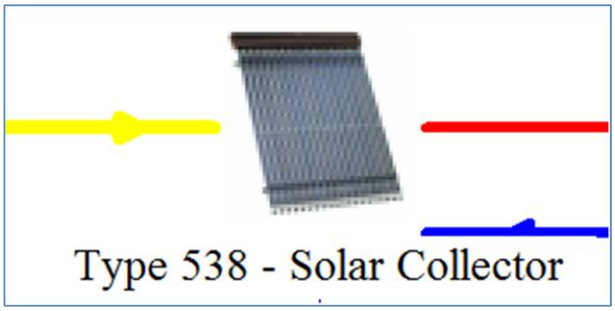

Figure 21: The icon used in TRNSYS for Type 538 evacuated tube solar collector

3.5 Collector Array Shading Component

Shading was not originally considered in the model. During the data review it was found that the model was outperforming the measured data, by an average of approximately 6% during the summer months and during the winter months by as much as 67%. One of the reasons for this outperformance was narrowed down to the possibility of shading, which should be greater in winter, when the solar azimuth angle is lower. With the height of 1,471mm and spacing of

5,100mm if the Sun's rays were lower than approx. 15° (due south) then there would be shading on the collector panels. With the introduction of the shading component the discrepancies were reduced.

Type 30 collector array shading component determines the incident radiation upon an array of collectors that shade one another. The model used for the component applies when the collector is set at a fixed angle similar to the setup at SLC. Geometrical angles are used to determine the angle at which the Sun's rays are interacting with the solar collectors and therefore an average value for the solar radiation is produced as the output.

Figure 22: The icon used in TRNSYS for Type 30 Collector Array Shading Component

3.6 Equation Component

The equation component is very important in TRNSYS as it can be used as a controller or as a calculator within the model. There are pre-programmed controller components in TRNSYS available, but for complicated or unique functionality as explained in Section 4.6 and Section 4.7 for the SLC model, it is easier to use the equation component. When being used as a controller, the logic algorithm must be set up in a manner that the only outputs possible are zero and one.

For the case of the SLC model, the Equation component was used to perform unit conversion and also as a controller for:

- the main system pumps (P1 / P2)
- the secondary loop for the domestic water heat tank, DWH5, pump (P3)
- the signal for the dry cooler, DC-1 that is used to prevent system overheat
- the three way diverting control valves for the heat exchanges

- the three way diverting control valves for the DC-1 or the DC-1 bypass

There are a number of logical functions that can be used in TRNSYS. The ones used in the SLC model are AND, OR and GT (greater than). The AND function has an output of 1; if, both the conditions listed within the function have the output of 1. The OR function has an output of 1; if either of the two conditions listed within the function have the output of 1. The GT function is used for comparison between different variables. To set this up, the function keyword is followed by a parenthesis in which there are two variables being compared. For example, if one variable (x) is greater than another variable (y) for the following logic:

$$Signal = GT\ (x, y) \tag{14}$$

Then the "$Signal$" variable will be set to 1 if $x > y$ and 0 otherwise.

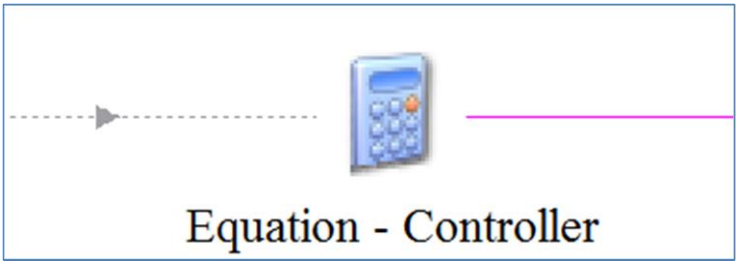

Figure 23: The icon used in TRNSYS for the Equation Component

3.7 Heat Exchanger Component

Heat exchangers are used to transfer heat from one working fluid to another. As discussed in Section 1.5, the working loop for the SLC solar heating system is a water and glycol mixture. The energy collected by the fluid externally must be transferred to water for it to be used within the SLC facilities.

The capacitance of the heat exchanger is not modeled within the TRNSYS component. The TRNSYS model uses the following formulas to calculate the temperatures of the hot side outlet temperature, T_{ho} and the total heat transfer across the heat exchanger, $\dot{Q}_T$;

$$T_{ho} = T_{hi} - \varepsilon_{HX}\left(\frac{C_{min}}{C_h}\right)(T_{hi} - T_{ci}) \tag{15}$$

$$\dot{Q}_T = \varepsilon_{HX}\, C_{min}\, (T_{hi} - T_{ci}) \quad (16)$$

where, T_{hi} is the hot side inlet temperature, ε_{HX} is the heat exchanger effectiveness, C_{min} is the minimum capacity rate, C_h is the capacity rate of fluid on the hot side calculated by using $\dot{m}_h C_{ph}$ ($\dot{m}_h$ is the fluid mass flow rate on the hot size and C_{ph} is specific heat of fluid on the hot side), T_{hi} is the hot side inlet temperature and T_{ci} is the cold side inlet temperature (Thermal Energy Systems Specialists, 2014). Capacity rate is the quantity of heat a fluid of a certain mass flow rate is able to absorb or release per unit temperature per unit time.

At SLC, two different types of heat exchangers are used to convert the energy collected by the water-glycol mixture into useful hot water.

3.7.1 Shell and Tube Heat Exchanger

Type 5g heat exchanger was used to model the shell and tube heat exchanger that is used to store the solar energy in the DWH5 tank. The energy from this tank is pumped to the DHW1 and DHW2 tanks. The DHW5 tank works as a heat exchanger as the water-glycol mixture is pumped through it at a higher temperature when the solar system is running.

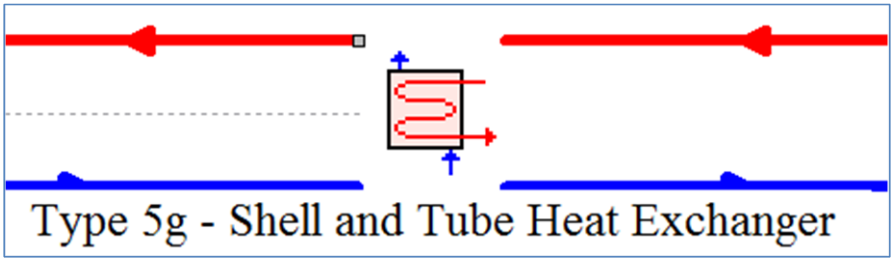

Figure 24: The icon used in TRNSYS for Type 5g Shell and Tube Heat Exchanger Component

3.7.2 Flat Plate heat exchanger

Type 5b flat plate heat exchanger was used to model the heat exchanger to transfer the heat from the water-glycol mixture to the make-up water. The flat plate heat exchanger has an advantage over other types of heat exchanger as it has good heat transfer, is easy to maintain, and is compact. Any time make-up water is brought into the facility and the solar system fluid has available heat energy, the flat plate heat exchanger is used to transfer the heat over to the make-up water.

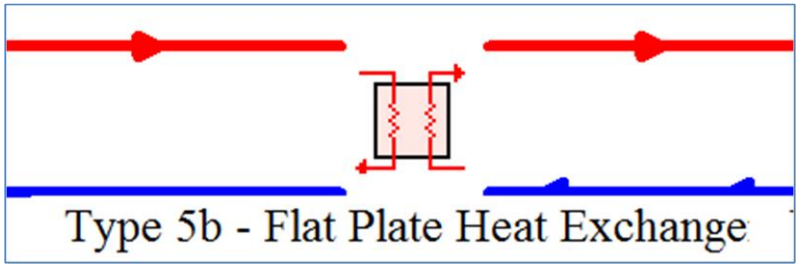

Figure 25: The icon used in TRNSYS for Type 5b, Flat Plate Heat Exchanger Component

3.8 Working Fluid Pump Component

For the main pump for the solar system, a Type 114 single speed pump component was used. This component does not model the pump starting and stopping characteristics. It ignores the mass flow rate as an input, except to perform mass balance checks. When setting up the simulation, extra caution must be exercised when specifying fluid loops between pumps and other components. The downstream flow rate is determined based on the flow rate parameters of the component and the control signal value. Cases when the inlet mass flow does not match the outlet mass flow are recorded on the list file at the end of each simulation (Thermal Energy Systems Specialists, 2014).

If the pump control signal is below 0.5, all output parameters, such as the mass flow rate and power drawn by the pump are set to zero. Any temperature outputs are all set to the inlet temperature. When the control signal is greater than 0.5, the pump is considered 'on' and the mass flow rate and power drawn by the pump are set to the rated conditions based on the component parameters, according to

$$\dot{Q}_{fluid} = \dot{P}_{shaft}\left(1 - \eta_{pumping}\right) + \left(\dot{P}_{rated} - \dot{P}_{shaft}\right) f_{motorloss} \qquad (17)$$

where the energy transferred from the pump motor to the working fluid is, $\dot{Q}_{fluid}$, $\dot{P}_{shaft}$ is the shaft power used for the pumping process, $\eta_{pumping}$ is the pumping process efficiency, $\dot{P}_{rated}$ is the total rated power of the pump and $f_{motorloss}$ is a fraction of the pump motor inefficiencies that contribute to a temperature rise in the fluid stream passing through the pump. Once the energy transferred to the working fluid is known, division by the mass flow rate gives the overall temperature increase of the fluid.

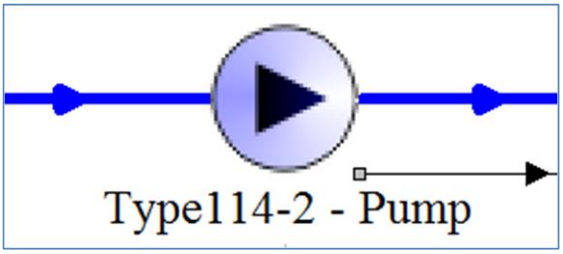

Figure 26: The icon used in TRNSYS for Type 114-2 Fluid Pump Components

3.9 Dry Cooler Component

A Type 511 component was used to simulate the dry cooler, which is located on the roof of the SLC to cool the water/glycol mixture if its temperature get too high. The hot fluid is passed through coils and fans are used to pass ambient air through the coils to lower the temperature of the fluid. In the dry cooler there is no direct interaction between the outside air and the fluid; this is a requirement at SLC as the fluid contains glycol which requires a closed circuit cooler. This component requires the user to provide the design parameters for the unit. It then calculates the overall performance of the device over non-design conditions. Even though the set-up of the component is simple, in the past, the component has been found to match the unit manufacturer's catalog data values (Thermal Energy Systems Specialists, 2012). The component assumes forced convection, as air passing over the coils containing the fluid. When setting up the component, the user has to provide:

- the design values for the fluid inlet and outlet temperatures
- the design fluid and air flow rate
- the design fluid specific heat
- the design air ambient temperature
- the rated power of the fan

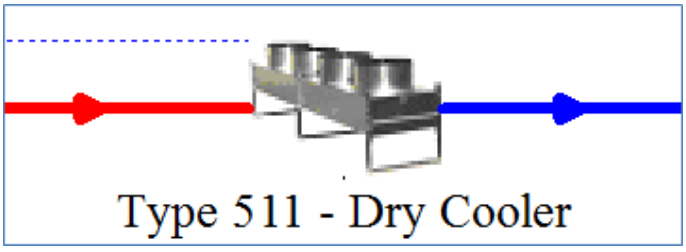

Figure 27: The icon used in TRNSYS for Type 551 Dry Cooler Components

4 Model Set-up

4.1 Overall Simulation Set-up

The components discussed in the previous chapter were connected together to form the TYNSYS model. The overall simulation was set up based on the information provided in this chapter and other relevant information.

The water that is heated by the solar system is further heated with gas boilers before being used within the SLC facilities and pool. The model does not simulate the system past the water going through the heat exchanger. All required energy transfer information is available at that point and there is no data recorded past this point in the Siemens Building Management System.

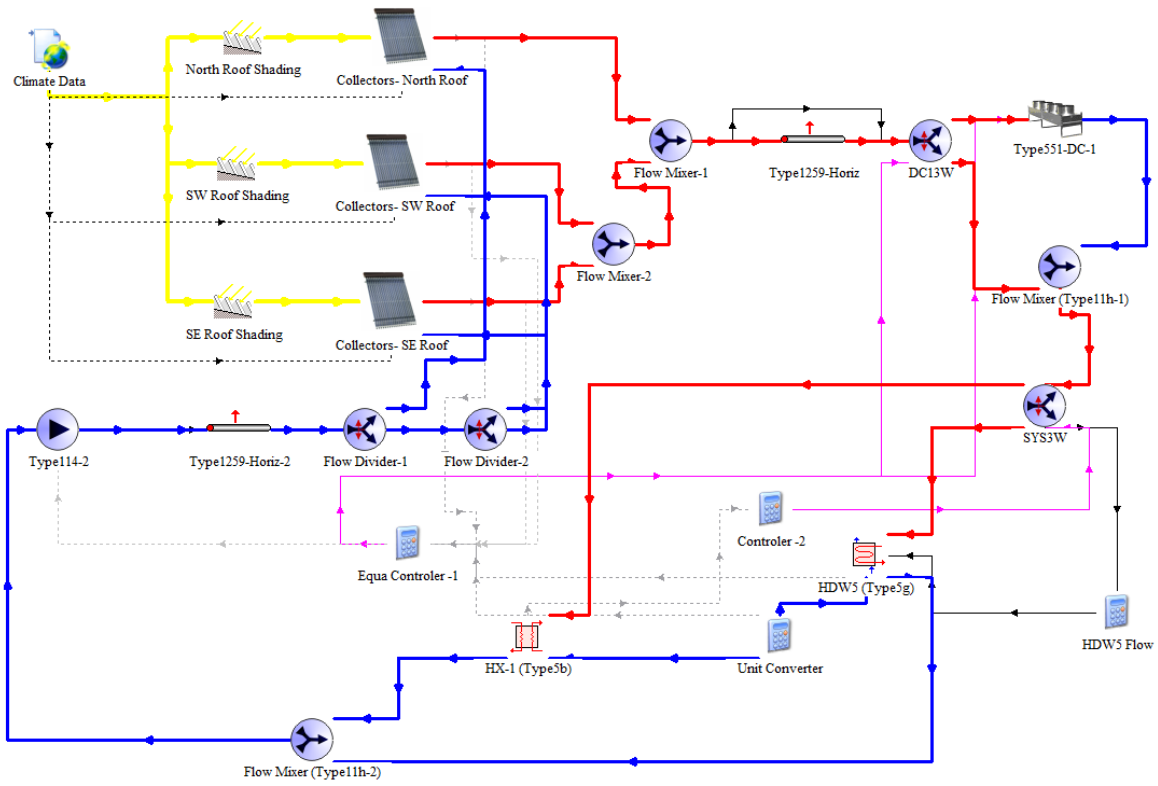

Figure 28: TRNSYS schematic of the SLC solar heating system

Figure 28 shows the schematic set-up in TRNSYS model including the different components and how they are connected together.

4.2 Parameters, Drivers and Outputs of the Model

As explained in Chapter 3, the program solves for all variables iteratively over the duration of the simulation. The user needs to define some basic principles, known as the 'control cards' information in TRNSYS, which the software should follow for it to successfully read the input files and perform the required tasks. The essential values that are entered by the user include the simulation start time, simulation end time and simulation time step. For the simulation the start and end time is the total number of hours past zero hundred hours from 1st January for any given year. This is the case as generic solar angular information has been used for the tracking of the sun. Also, due to unavailability of data, explained further in section 5.1, the simulations for any given day have to start at 2:15 AM and end at 11:45 PM on the same day. For example, if the simulation was for the 2nd of January, the start time would be 26.25 hours (24 + 2.25) and the end time would be 47.75 hours (24 + 23.75). The data collected by Nadeekangani (2014) was recorded ever minute; however, the Siemens Building Management System only recorded every 15 minutes. Even though a smaller time step was preferred, the solar collector simulation time step had to be set for 15 minutes. There are also other project specific parameters related to warning, number of iterations and tolerances that are specified by the user in the control card.

For the SLC solar model there are a number of drivers that provide the required information for the simulation to run for the entire day. If even one of these simulation drivers is missing for a small duration during the day, then the simulation does not have the essential information needed to be able to calculate the performance of the system. The input drivers of the SLC TRNSYS model include:

- The orientation of the Sun to the solar panels and ground
- The amount of solar radiation available
- The ambient temperature
- The make-up water temperature and flow rate
- The inlet temperature of the shell and tube heat exchanger

The outputs from the model can be changed to what is required by the user easily. The Type 65 plotter has been utilized extensively for this study. The plotter is used to display variables that have been selected by the user while the simulation is processing. This way the user can immediately see any deviation from what is expected, stop the simulation, and make appropriate changes before restarting the simulation. For the case of this simulation, although temperatures and control signals of almost every component are plotted, the main point of interest is the overall energy that is transferred from the two heat exchangers to the domestic water. This can also be referred to as useful energy for the solar system at SLC.

4.3 Solar Collector Set-up and Validation

Before the complete model was built, the panels were simulated for the conditions of the Fraunhofer tests to establish the accuracy of their modeling. With the Type 538 model the inputs and outputs are set in a manner that the model does not consider the wind speed and additional heat losses due to wind. That does not mean that the wind does not affect the collector performance, but that the available TRNSYS models do not have the capabilities to include wind speed in their heat loss calculations. The parameters for the collector were obtained from manufacture's specifications and the tests performed on the solar collector by Kramer (2007). The test value that was entered in the TRNSYS parameters was one of the runs performed during the testing to calculate the efficiency coefficients. The parameters used for the Type 538 solar evacuated tube heat collector can be seen in Figure 29.

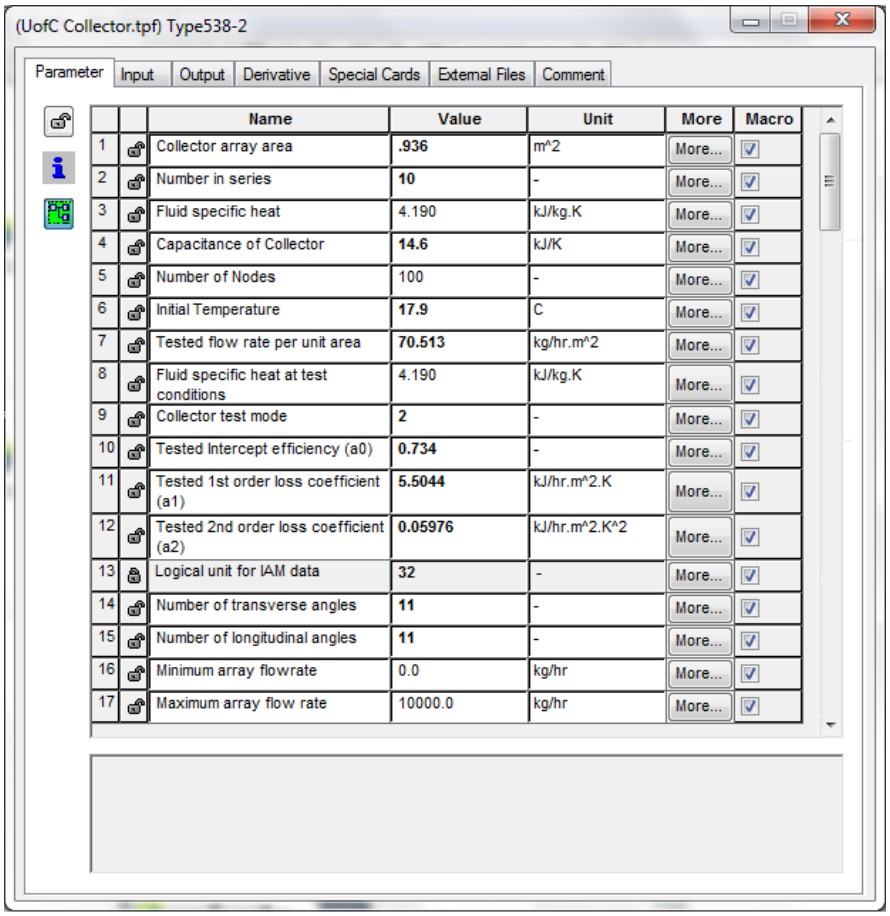

		Name	Value	Unit	More	Macro
1		Collector array area	.936	m^2	More...	☑
2		Number in series	10	-	More...	☑
3		Fluid specific heat	4.190	kJ/kg.K	More...	☑
4		Capacitance of Collector	14.6	kJ/K	More...	☑
5		Number of Nodes	100	-	More...	☑
6		Initial Temperature	17.9	C	More...	☑
7		Tested flow rate per unit area	70.513	kg/hr.m^2	More...	☑
8		Fluid specific heat at test conditions	4.190	kJ/kg.K	More...	☑
9		Collector test mode	2	-	More...	☑
10		Tested Intercept efficiency (a0)	0.734	-	More...	☑
11		Tested 1st order loss coefficient (a1)	5.5044	kJ/hr.m^2.K	More...	☑
12		Tested 2nd order loss coefficient (a2)	0.05976	kJ/hr.m^2.K^2	More...	☑
13		Logical unit for IAM data	32	-	More...	☑
14		Number of transverse angles	11	-	More...	☑
15		Number of longitudinal angles	11	-	More...	☑
16		Minimum array flowrate	0.0	kg/hr	More...	☑
17		Maximum array flow rate	10000.0	kg/hr	More...	☑

Figure 29: Parameters of the Type 538 solar collector used for simulation

To verify the collector model, the radiation, flow rate, inlet and ambient temperatures that were measured during the testing were used in TRNSYS; the intent was to duplicate the testing to see if the predicted output temperatures would match the measured values. Table 4 shows the three different values that were used in the simulating when comparing the results with tests completed in Germany.

Table 4: Table showing the values used for the collector testing in TRNSYS **(Kramer, 2007)**

Solar Radiation (W/m^2)	Flow Rate (kg/hr)	Inlet Temperature, T_{in} (°C)	Outlet Temperature, T_e (°C)	Ambient Temperature, T_a (°C)
980	67.7	6.79	15.38	9.88
921	65.9	33.26	40.87	9.85
991	65.2	85.50	91.65	9.31

The overview of the TRNSYS schematic can be seen in Figure 30. A Type 65d plotter was used to show the results. The above mentioned radiation was used as a constant and the temperatures were recorded once the system had reached steady state solution.

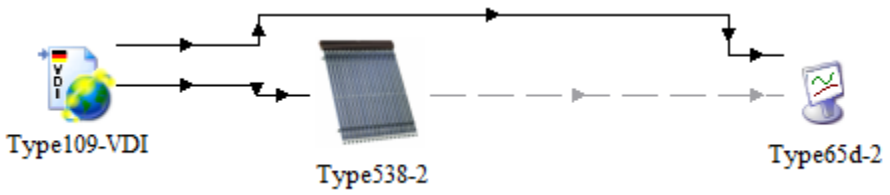

Figure 30: The overview of the schematic used for the collector testing

The difference in the temperature between the experimental measurements and TRNSYS simulated outlet temperatures are shown in Table 5.

Table 5: Results from comparing measured and simulation exit temperature difference

Measured T_{out} (°C)	Simulated T_{out} (°C)	Percentage Difference (using T_e - T_{in})
15.38	15.31	0.81%
40.87	40.86	0.13%
91.65	91.69	-0.65%

The measured and simulated values were found to be within the acceptable range and the solar collector model was considered to be a fair representation of the solar collectors used it SLC. As the pyranometers used has an average daily accuracy of 10%, a margin of error of 5% between the measured and simulated exit temperature difference was considered within the acceptable range (Nadeekangani, 2014). Even though the total solar beam radiation was set equal to the Fraunhofer test values, no diffused radiation was used to verify if this would be satisfactory for modeling the SLC solar collectors. This was done as the measurements taken at SLC in Calgary were only of the total radiation. It is therefore assumed that the diffused radiation alone in the TRNSYS Type 538 component does not significantly affect the performance of the evacuated tube solar collectors.

4.4 Accounting for Solar Shading

Due to the latitude of Calgary, the Sun is never directly overhead. The solar collectors at SLC were set at 45° tilt but due to proximity to each other, they can experience some solar shading at certain times of the day and year. Although this is not significant in the summer months, during the winter months when the solar zenith angle is high, the shading can affect the output of the solar collector. During this research, the losses due to shading were considered as part of the system losses. The schematic of a basic solar model using the solar shading component can be seen in Figure 31.

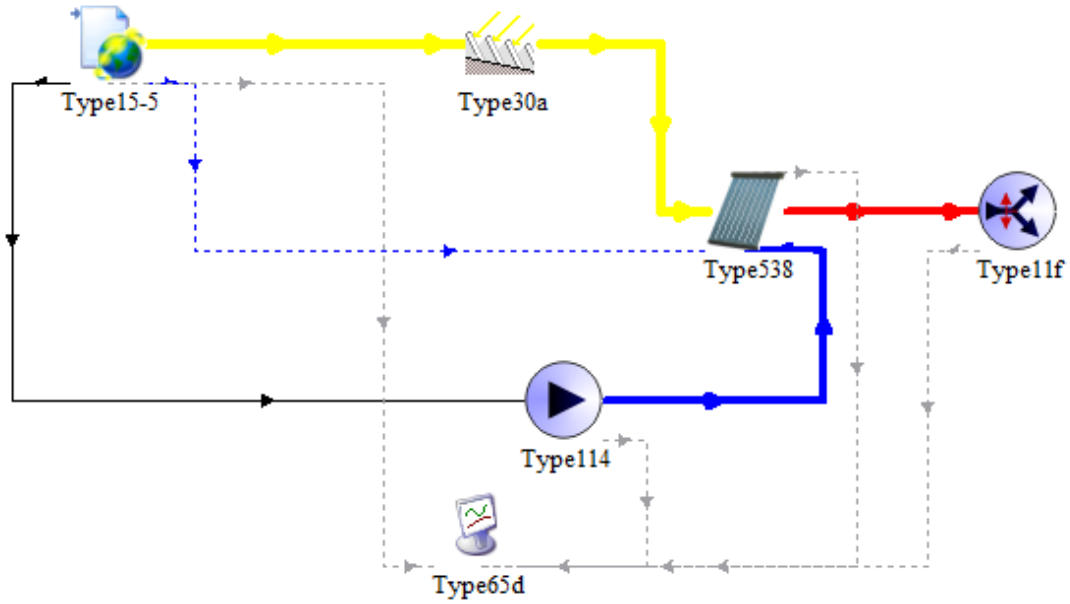

Figure 31: Schematic of a basic setup for a model using the solar shading component

Solar shading can cause dramatic loses in photovoltaic power output. Even though solar shading does not cause a dramatic decrease in heat output for solar heat collector, it should still be considered. The Type 30a solar shading calculator tool determines the average incident radiation on an array for connectors that shade each other. The parameters for the case of the north roof can be seen in the figure below. The data used was derived from the engineering drawings used during the assembly of the heat collectors.

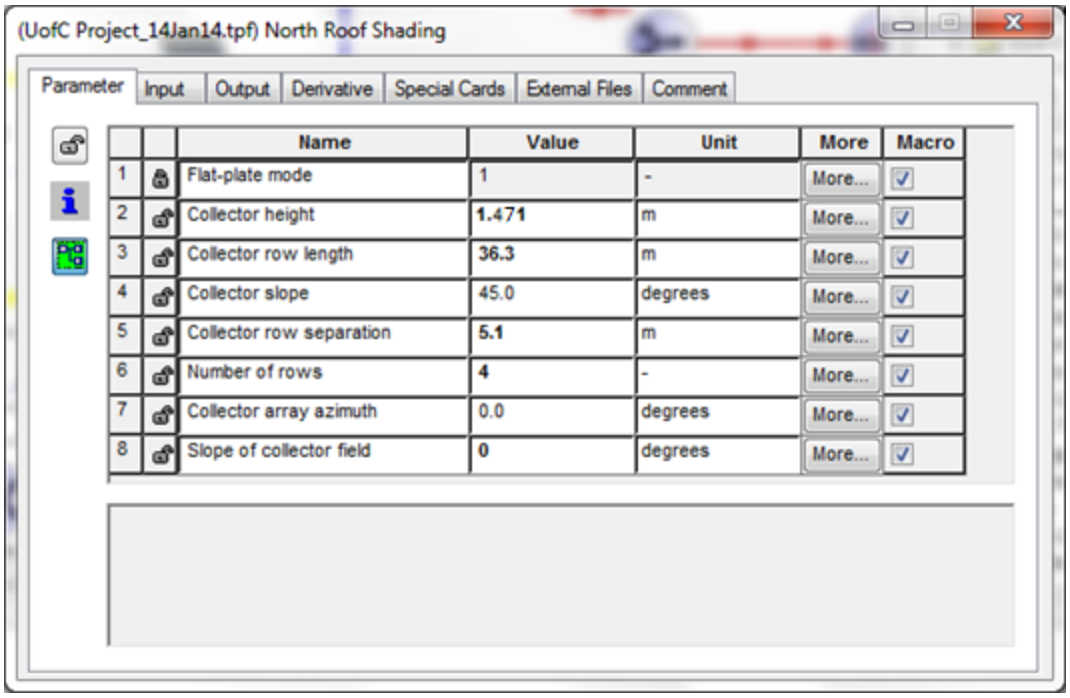

Figure 32: Values used to set up the shading component

4.5 Heat Exchanger Model

As stated earlier, there are two fluid heat exchangers within SLC's solar heating system. When the solar system is activated, the water-glycol mixture returning from the solar collector is sent to one of the two exchangers. There is a three way diverting valve, SYS 3W shown in Figure 28 (as are all the following components denoted by abbreviations), that is used to direct the flow, either through the shell and tube heat exchanger, DHW5, or the flat plate heat exchanger, HX-1. The input signal to the valve is based on where the heating is required. If there is cold inlet make-up water flow through HX-1, then the hot water-glycol mixture is also directed to HX-1. If there is no make-up water flow through HX-1, then the flow is directed to DHW5.

4.5.1 Shell and Tube Heat Exchanger Set-up

Type 5g, zero capacitance shell and tube exchanger was used to reproduce the HDW5 heat exchanger in the TRNSYS model. The overall heat transfer coefficient of the heat exchanger was calculated by performing iterations in the simulation software. To mimic the design conditions for the heat exchanger, the source inlet was set to 94°C and load inlet at 10°C. The transfer coefficient was changed so that the outputs were equal to 76°C and 60°C respectively. The

exact output temperatures were not achieved as the source fluid did not have enough heat energy available. The transfer coefficient used provides the resulting temperatures very close to design temperatures. The values used for the specific heat of water and water-glycol mixture can be seen in the Figure 33. After review it was determined that the heat exchanger design conditions were inaccurate; however, as the error was minor, so it was ignored (further elaborated in Section 4.8).

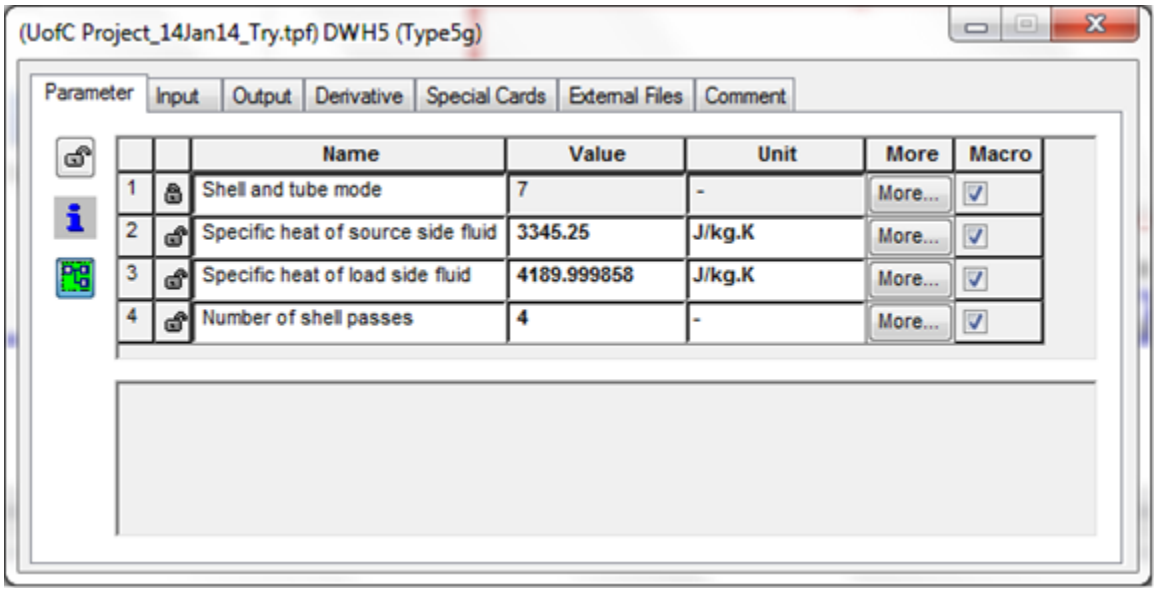

Figure 33: Specific heat values used for DWH5

4.5.2 Flat Plate Heat Exchanger Set-up

As stated earlier, Type 5b, zero capacitance counter flow flat plate heat exchanger was used to represent the HX-1 heat exchange in the TRNSYS program. The overall heat transfer coefficient of the heat exchanger was calculated by iteration (similar to DWH5). The source inlet was set to 94°C and load inlet at 10°C, the transfer coefficient was changed so that the outputs were equal to 76°C and 30°C respectively. The calculated transfer coefficient used can be seen in Figure 34.

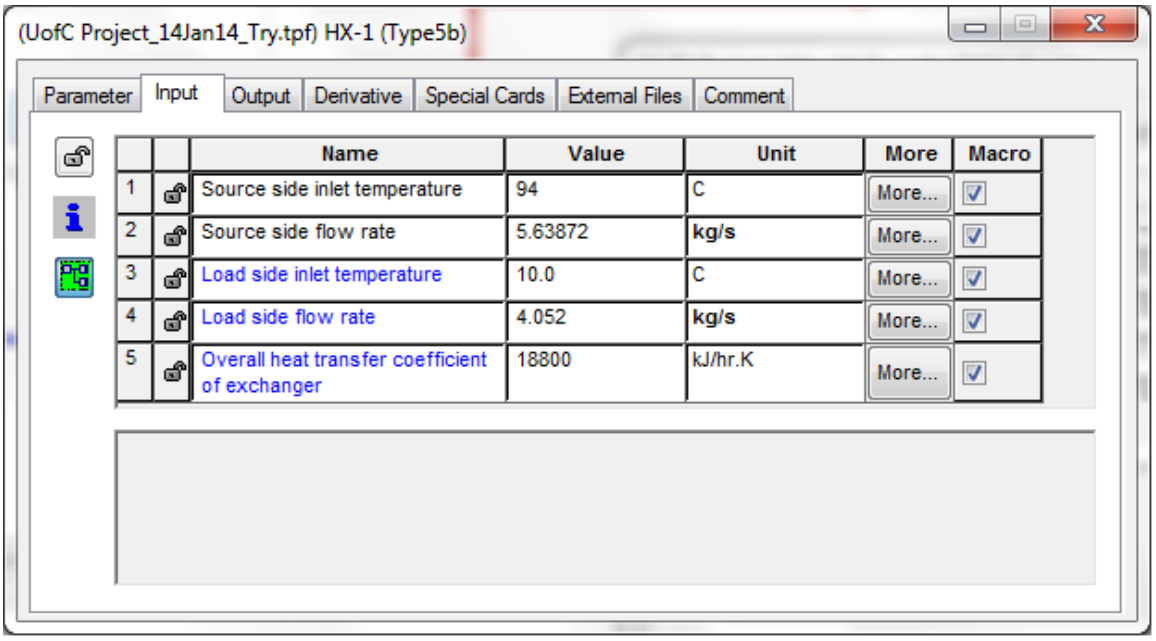

Figure 34: Heat transfer coefficient for HX-1 Heat exchanger

4.6 Pump and Pump Controller Set-up

The water-glycol mixture is pumped through the solar collectors and the heat exchanges using a hydraulic pump (P1 / P2). The power rating of the pump is 5.6 kW. The flow rate achieved by the pump is 5.36 liters per minute. A Type 114 component was used to simulate the pump in TRNSYS. The rating and flow of the pump was set to the design conditions. The flow through the main loop of the system is set based on the flow rate specified in the pump parameters. Two different pumps, P1 and P2, were installed in parallel for redundancy in case of equipment failure. Only one of the two pumps can run at any given time.

The pump is controlled with multiple sets of conditions, when satisfied turn the pump on or off. The TRNSYS component used as a controller has a signal output of 1 when the pump is to be turned on and 0 when pump is to be turned off. As per the TRNSYS model set-up, the pump would operate if:

- The average solar collector temperature, T_{avg} is 5.5 °C greater than the DWH5 tank temperature, $DHW5T$ and $DHW5T$ is below 60 °C

- Or, there was flow measured on the make-up water side through HX-1, $HXFlow$ and the average temperature of the solar collector was greater than the inlet make-up water temperature, $HX1MUT$ by 5.5 °C
- Or, the average solar collector temperature was greater than 89 °C.

4.7 Dry Cooler Set-up and Controller

The purpose of the dry cooler is to ensure that the heat collectors, water-glycol mixture and other components of the system do not get damaged due to the excessive temperature. The flow is directed to the dry cooler if the system does not require any additional heat and the average heat collector manifold temperature goes above 94°C, or if the system is requesting heat and the average heat collector manifold temperature goes above 96°C. As stated in the manufacturer's specification, each fan has an air flow capacity of 10,000 cubic feet per minute. The design conditions provided by the EPC Company were used for the TRNSYS model; the parameters used can be seen in Figure 35.

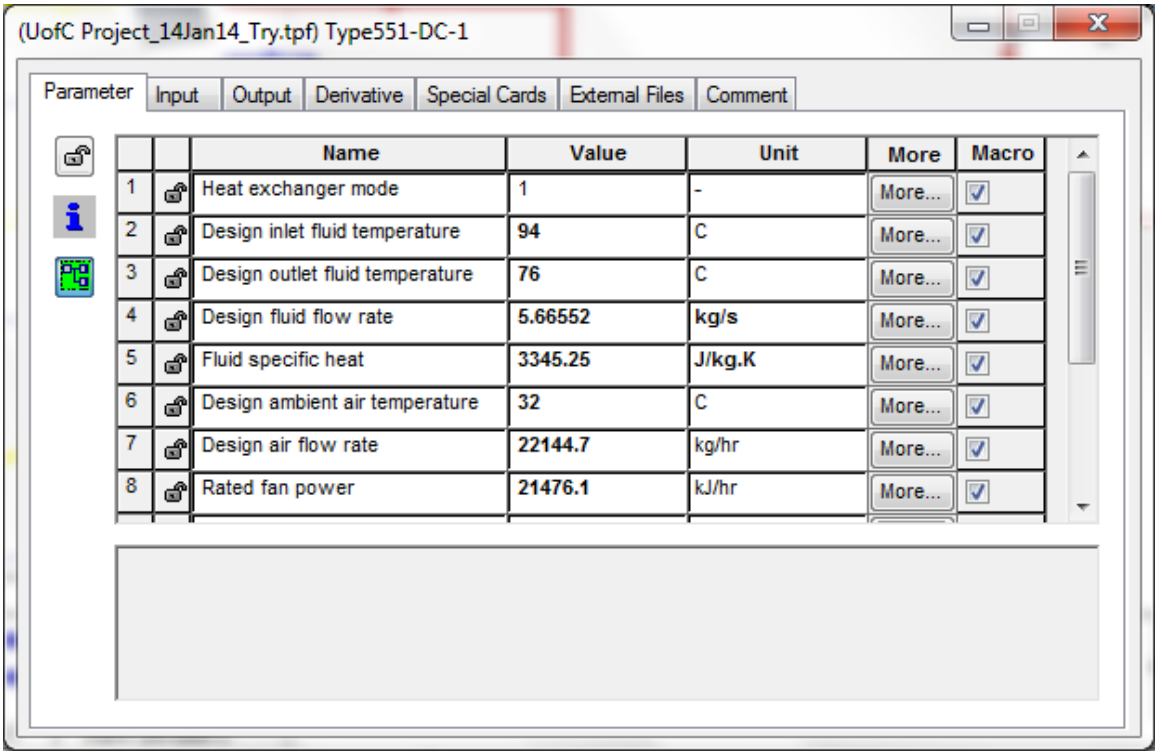

Figure 35: Parameters used for the dry cooler design condition

DC-1 3W is the three way diverting valve that is used to direct the flow either through DC-1 or to bypass DC-1. The input signal to the valve is based on whether the system is asking to cool the water- glycol mixture. The conditions for the controller to direct flow to DC-1 and turn DC-1 'on', DC_{Signal} are:

- The $DHW5T$ is greater than 60 degrees; there is no flow through the flat plate heat exchanger ($HXFlow$ equal to zero) and T_{avg} is greater than 94 °C
- Or, T_{avg} is greater than 96 °C

The condition of when the dry cooler should start has been duplicated well between the simulation and actual controller set-up as they have the same start conditions. The problem is for when the dry cooler should turn 'off'. In the simulation, as soon as the conditions stated above are not satisfied, the dry cooler will turn off. In the actual system, if the heat is not needed elsewhere the dry cooler will continue to run until the fluid temperature reduces to 50°C. If the dry cooler was started because of the fluid temperature reaching 96°C, then the dry cooler would continue to run, even if the system is asking for heat, until the fluid temperature reaches 65°C. Once the dry cooler turns on the simulation cannot fully duplicate the actual measured conditions.

4.8 Limitations and Assumptions of Model

Attempts were made to make the model as realistic as possible. During the development of the model, there were a number of assumptions that had to be made and there were a number of limitations that were discovered. Some limitations were resolved, but a few still remain in the model. It is important to be aware of these limitations, as some of them could not be resolved based on the data available and others were not resolved in the time available. The important limitations are listed below.

Supply and return piping for the internal and external loops

The piping to and from the solar collector are different lengths and diameters, depending on which solar array the fluid is going to or returning from. If this was considered for each solar

array, there would be 50 different piping components required for each supply and return loop. This would also mean that there would have to be 50 solar collector components in the model. Instead of proceeding with such high number of components an approximate length of 150m of piping was assumed for each supply and return loop. This approach reduces computational time and on a macro basis should not affect the overall system performance. Piping heat loss parameters were updated iteratively and comparing results to make sure that the pipe was a good representation of the actual piping. Small length piping within SLC was not considered, as the heat losses would be negligible due to higher facility temperature and minimal lengths.

Wind direction and speed

Losses due to wind direction and speed were not considered in the model. Even though TRNSYS can manage the additional algorithm required for wind effects, the solar collector component used, Type 538, does not have the capability. Thermal Energy System Specialists, the developers of TRNSYS, were contacted in regard to incorporating wind losses in the component but they required funding to be able to spend time to include the added complexity for the component. Also, additional testing would need to be performed on the type and model of solar collector being used, as new efficiency curve would have to be developed that consider solar radiation, wind direction, wind speed and ambient temperature. Currently, the component uses the efficiency curve which considered solar radiation and difference between the fluid and ambient temperature, Equation (10). This was considered to be a limitation of the current model for this research. The standard EN 12975, on which the tests were based, has no limitation on wind speed (Kovacs, 2012) but it was noticed that during the thermal testing the evacuated tubes were subjected to a mean wind speed of only 3 m/sec (Kramer, 2007).

Cold weather experienced in Calgary

During the testing at the Fraunhofer Institute, the lowest ambient temperature the tests apparatus were exposed to was 6.9°C (Kramer, 2007). During the study at SLC the lowest ambient temperature was -21.2°C; it is assumed that the efficiency curve is valid for lower temperatures. Similar to wind speed, the testing standard EN 12975 does not list a minimum or maximum temperature requirement (Kovacs, 2012).

Time step of 15 minutes used in the simulation

The recorded solar data was taken every minute. This is a good time step as the main system pump can be 'on' for a minimum of 10 minutes. The Siemens building monitoring system had a recording frequency of 15 minutes. Due to this, the simulation time step had to be increased to 15 minutes. The alternative of increasing the building data recording frequency was explored, but due to budgetary constraints was not done. Also, majority of the data had already been collected and exploring it further would have meant ignoring the already collected data.

Dry cooler turn off mechanism

As discussed in Section 4.7, the dry cooler was set up to turn off as soon as the turn on conditions were not applicable. This was not how the actual SLC system conditions was set-up but as once the dry cooler turns 'on' the additional complexity involve make it very hard for the simulation to be able to duplicate the actual conditions.

DHW5 design conditions

As discussed in section 4.5.1, DHW5 was modeled using the design conditions. After further examination of the design conditions and the specific heat of water, load side and water-glycol mixture, source side, it was realized that the design conditions were not correct and the data were inconsistent with the law of conservation of energy. Best fit values for the heat exchanger heat transfer coefficient was used and the margin of error was small enough (2.9% heat energy difference) to be assumed to be negligible for the overall results.

Heat exchanger capacitance

Due to the type of TRNSYS components available, the heat exchangers used for the simulation had zero capacitance; this is a limitation when compared to the actual heat exchanger. This was not a major concern, as this made it easier to calculate the total energy derived from the solar system and should not add significant error.

DHW1 and DHW2 data

The temperature and capacitance data from the DHW1 and DHW2 tanks was not available from the Siemens building system and was not considered. As the energy stored in these tanks is directly available for use to heat the pool or to be used in the building facilities, it was determined that they can be considered out of the scope of this study.

In operation, as DHW5 collects more heat, the temperatures of the other two tanks would also rise. This could in turn cause the inlet temperature to DHW5 to go up. This was indirectly considered, as an actual temperature reading of the inlet temperature to DHW5 was used in the simulation. The problem is when the design conditions were changed, as this could in turn change the DHW1 and DHW2 temperatures and effect the inlet temperature to DHW5. This would, to a certain degree, change the overall system performance. This could not be considered in the simulation as the load on DHW1 and DHW2 was not recorded and neither were the initial start of simulation conditions.

The effects of these assumptions and limitations were considered to be negligible or out of the research's control. It is expected that these should not significantly affect the system performance.

5 Discussion

5.1 Quality of Data

The data was collected continuously between 7th March 2013 and 4th March 2014. During this time, all the variables required for the simulation were to be recorded. The intent was to run the TRNSYS simulation continuously over a span of a few weeks or months. While performing spot checks, it was realized that the data recorded from the Siemens Building Management System had missing information; during these instances, the data was not being stored and the program was recording only a 'Data Loss' error message. This was originally assumed to be a one-off error, but when it persisted, it was raised to the City of Calgary engineers for resolution. The error was not pursued by the City of Calgary, the owner and operator of SLC. Due to the data loss, the simulation could not be continuously run for a long duration; the available data limited the runs to a maximum of two continuous days. Out of the data sampled for 363 days, only 72 days did not have the 'Data Loss' error.

The remaining data was spot checked to confirm acceptability. When the data was set-up to be used in the simulation, it was discovered that the solar data recorded by Nadeekangani (2014) had some inaccuracies. Due to this, the number of days the simulation could be run was reduced from 72 to 30. As an example, for the 17th of July, 2013, the solar radiation during the night was recorded to be 1.24 kW/m^2; similar discrepancies were found for daytime and nighttime. 1.24 kW/m^2 is higher than the expected solar radiation for a clear sunny summer day. During the setup of the final simulation drivers, it was determined that the 'Data Loss' error also existed for the building flow meters. As a result, the final number of days for which all the required data was valid and available was 15 non-consecutive days.

Table 6: Dates for which complete data set was available

Day of month	Month and year
2, 9, 16	June 2013
4, 11, 18, 25	Aug 2013
1, 8	Sept 2013
1, 8, 15, 22, 29	Dec 2013
12	Jan 2014

As a result of the data loss, each day the simulation starts at 2:15 am and ends at 11:45 pm. As per the manufacturer's specifications of the pyranometers, the solar radiation measured over the period of a day is expected to have an accuracy of $\pm$ 10% (Nadeekangani, 2014). The inaccuracy of the pyranometers and other measurement devices, influence the results from the simulation.

5.2 SLC Overall Natural Gas Consumption

As the project was in collaboration with the City of Calgary, the natural gas consumed by the SLC from 2009 to 2012 was made available. The solar heating system was installed at the SLC during 2011. Gas consumption from Southland Leisure Centre from July 29, 2011 onwards can be seen in Figure 36. The data is plotted starting on July 29th of each year for the next 240 days for three consecutive years. Surprisingly, the natural gas usage at SLC has been increasing year over year, including after the installation of the solar collectors.

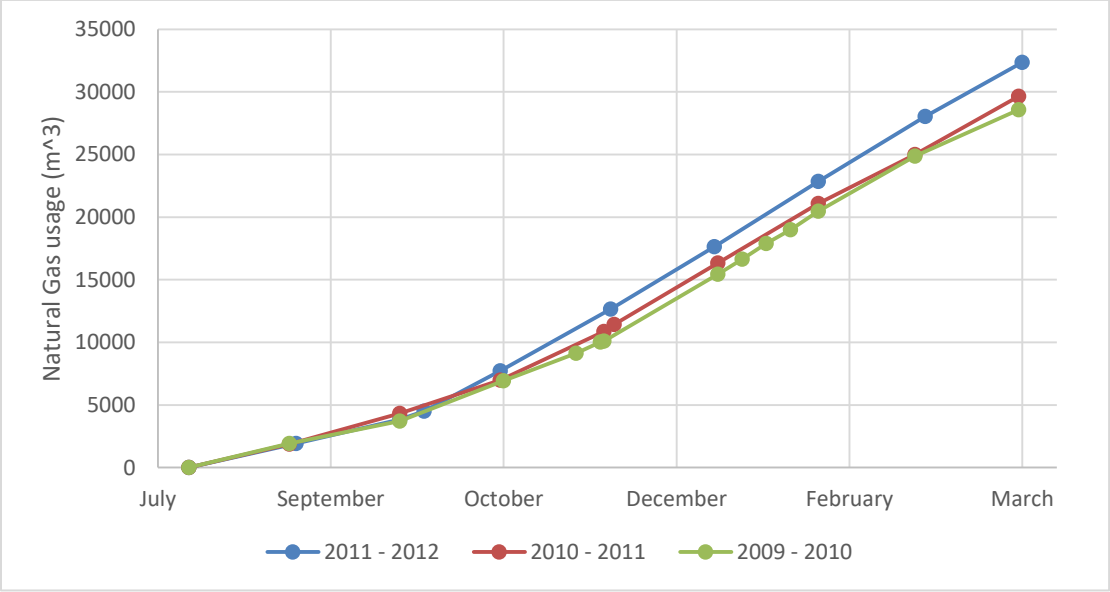

Figure 36: Natural Gas Usage at Southland Leisure Centre

The deviation from the expected reduction in natural gas consumption at SLC could be due to:

- Possible additions to SLC that could have increased the overall heat requirement

- As the City of Calgary grows, so does the membership of all the recreational facilities including the Southland Leisure Centre. Added members could increase the overall facility heating requirements
- The operational hours and system settings might have been changed, causing additional heat load. Solar energy harvested was not significant to reduce gas consumption.
- The installation of the solar collectors and changed operational conditions could affect the overall efficiency, causing increased use of natural gas
- Outside weather conditions fluctuate every year. This could result in higher natural gas consumption

With the increased gas consumption, extra care was used when determining the energy saved from to the installation of the solar collectors.

5.3 System and Simulation Performance for Summer Months

Out of the fifteen days for which the simulation was run, there were nine days from summer (including late spring).

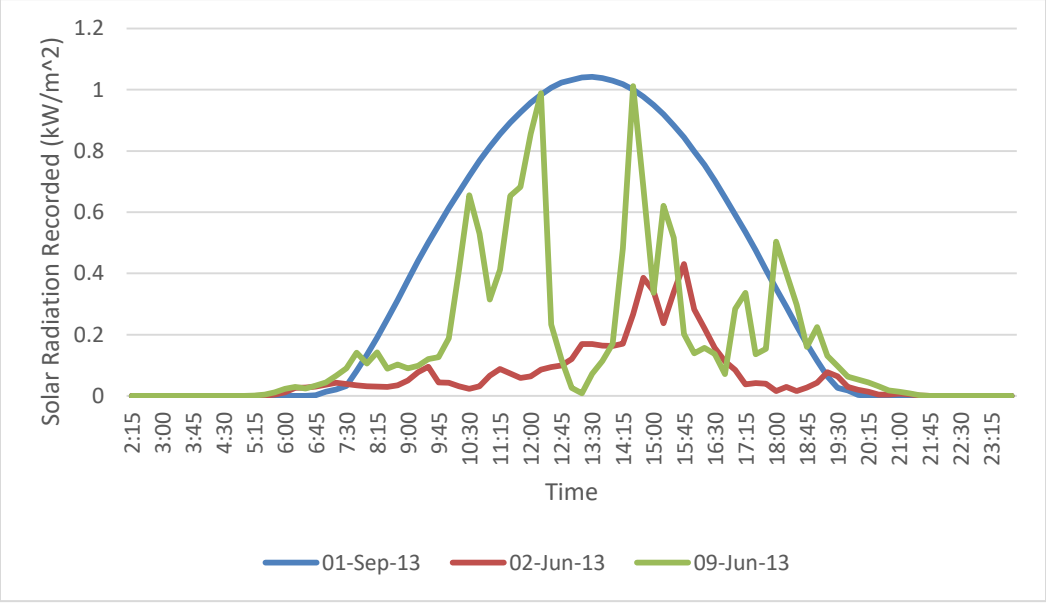

Figure 37: Solar radiation recorded for three days during summer 2013

The solar radiation recorded for three of the summer days is shown in Figure 37. The radiation for 1 Sept, 2013 indicates almost no cloud cover. The data recorded for 9 June, 2013 shows partly cloudy conditions, and for 2 June 2013 the weather conditions are overcast for almost the entire day. These conditions give the researcher the opportunity to duplicate a few different type of summer weather conditions that can be observed in the Calgary area. For the nine days the simulation was performed, the solar energy available during the day varied from 2.2 GJ per day to 11.8 GJ per day. Solar energy available is the overall solar radiation projected over the entire area of the solar array assuming there is no solar shading. The results show how local weather conditions can cause a varying range of solar radiation.

Table 7: Explanation of legends in Figure 38, Figure 40, Figure 42, Figure 43 and Figure 43

Legend in Figure	Explanation
Temp Solar in	Temperature of working fluid entering solar array
Temp Solar out	Temperature of the working fluid exiting solar array
Temp IN HX/DHW5	Temperature of the working fluid entering one of the two heat exchangers (same temperature)
Temp_Load_DHW5T_Out	Temperature of the working fluid exiting the shell and tube (DHW5) heat exchangers

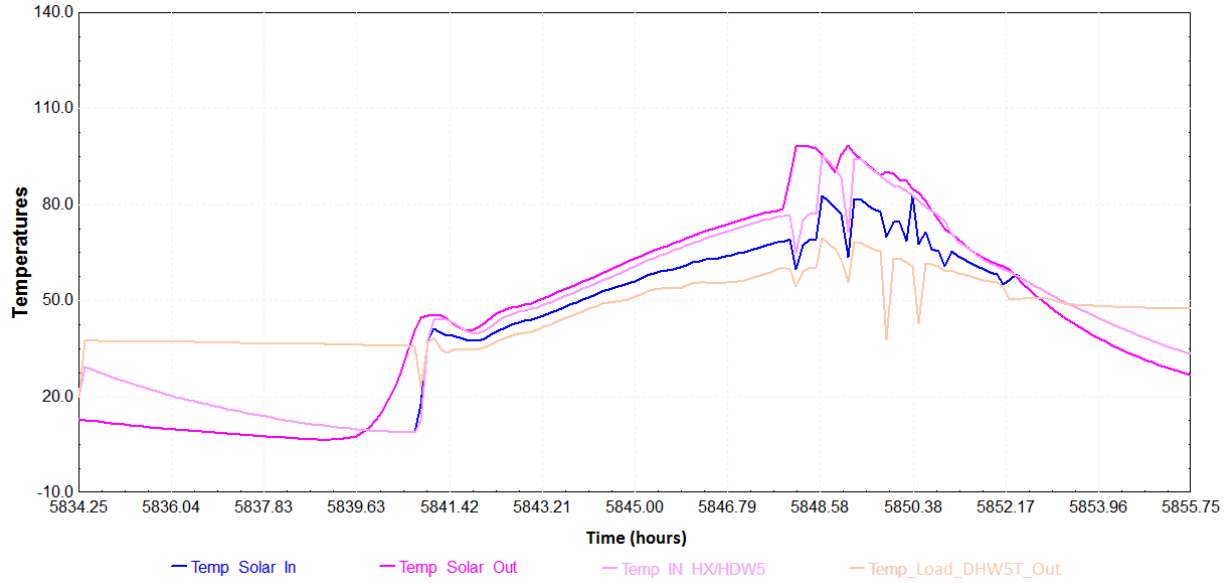

Figure 38: Simulation output graph for 1 Sept, 2013 (temperature in °C)

The output of the simulation for 1 Sept, 2013 can be seen in Figure 38. The simulation is for the entire day and it can be noticed that the temperature of the fluid exceeded 96°C. During these

conditions DC-1 is turned on and the fluid is circulated through the system until the fluid temperature drop below 65°C. Although the water-glycol mixture temperature is not measured in the building heat management system, the simulation indicates that the temperature does get higher than 94°C and that DC-1 should be turning on to expel the heat from the system to the environment.

Table 8: Data from the summer simulations performed

Date of Simulation	Average Ambient Temperature (°C)	Solar Energy Available (kJ)	Measured Harvested Energy (kJ)	Simulation Harvested Energy (kJ)	Simulated Total Pump Power Used (kJ)
01-Sep-13	18.1	11,788,832	1,783,643	4,633,300	214,200
02-Jun-13	9.4	2,160,200	753,386	1,327,000	166,320
04-Aug-13	15.7	5,776,674	2,930,623	2,427,300	191,520
08-Sep-13	14.4	9,446,926	948,259	2,203,400	171,360
09-Jun-13	11.9	5,724,335	1,935,048	2,611,000	204,120
11-Aug-13	19.6	10,349,920	5,506,936	4,907,100	249,480
16-Jun-13	15.4	9,704,827	4,091,619	3,985,800	221,760
18-Aug-13	21.3	11,383,166	5,227,345	4,772,300	236,880
25-Aug-13	19.4	6,097,350	2,294,756	1,884,400	209,160

Table 8 shows the simulation results summary for the summer days. For 1st and 8th September, 2013 data was not used to evaluate the system as the DC-1 turns 'on' during the simulation and as already discussed, the control mechanism for the simulation and the actual pump are different. The results and examination of simulation charts in detail (similar to one in Figure 38 for all simulations and variables) show a number of trends that will be explored in more detail throughout this Chapter 5. During hot summer days, when the make-up water is not turned 'on', a high quantity of heat is exhausted into the environment. This explains the low measured efficiencies for days when the fluid temperature exceeds 94°C. During summer months, there are a number of occasions where the solar heat is readily available, but the water temperature in the storage tanks is already at 60°C, in which case the system turns off. When the temperature is close to 60°C, the heat transfer at DHW5 slows down. It was noted that DHW5 is not performing at the same capabilities as design / simulation conditions; this is explained in

Section 5.9. Underperformance of DHW5 causes slower than anticipated heat transfer between the water-glycol mixture and the hot water storage tank. Also, it was noted that the make-up water feed was often turned on at 7 am. This is not the ideal time to try to harvest heat from the solar radiation during summer months.

5.4 System and Simulation Performance for Winter Months

Out of the fifteen days for which the simulation was performed, there were six winter days.

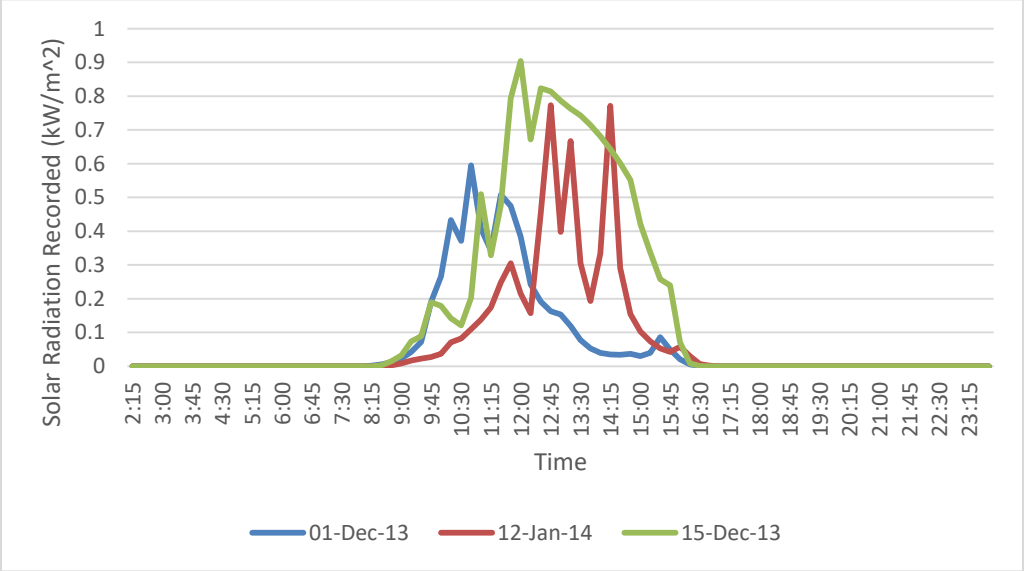

Figure 39: Solar radiation recorded for three days during winter 2013-2014

The solar radiation recorded for three of these days is shown in Figure 39. The radiation for 15th December 2013 was not obstructed during most of the day. The data recorded for 12th January 2014 shows partly cloudy conditions and for 1 December 2013 the weather conditions are overcast for almost the entire day. Similar to the summer days, these give the opportunity to simulate different weather conditions.

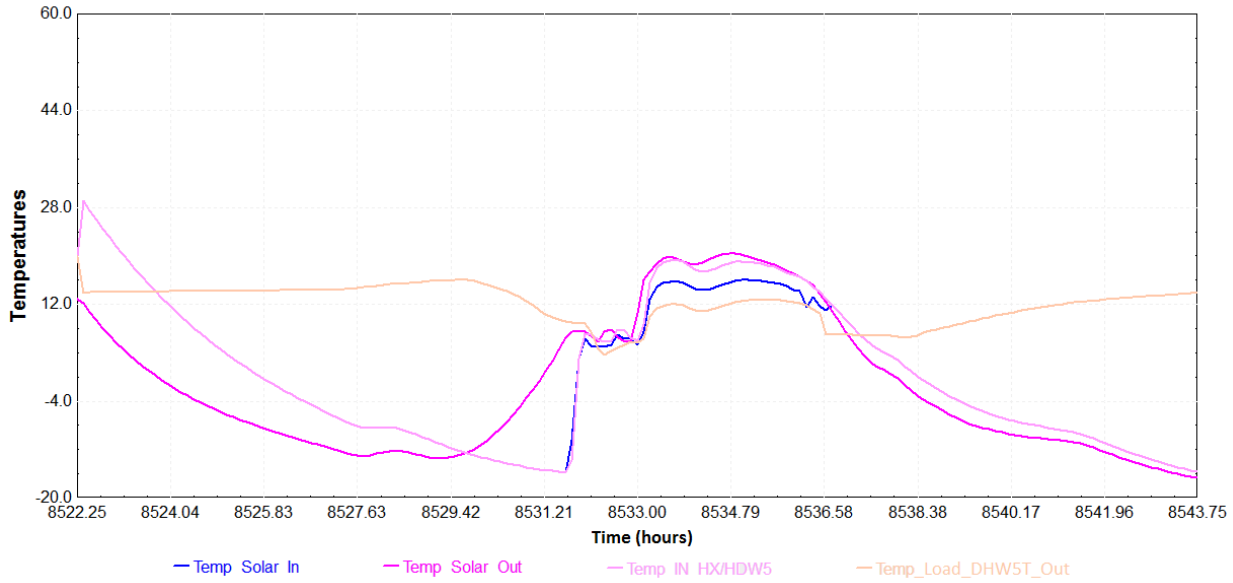

Figure 40: Simulation output graph for 22 December, 2013 (temperature in °C)

The output for the simulation for 22nd December 2013 can be seen in Figure 40. The simulation is plotted for the entire day and a very interesting phenomenon is noticed during the start-up on the system. Between 8,531.50 hr and 8,531.75 hr (9:15AM - 9:30 AM) it was noticed that when the system turns on, the solar heating system was actually cooling the make-up water. This was confirmed after examination of the measured data, which showed the cooling continued for more than an hour. This is due to heat loss from the water-glycol mixture as it travels between the solar collector and the building interior. The highest temperature of the water-glycol mixture for the simulation during the 6 winter days was 33°C.

Table 9: Data from the winter simulations performed

Date of Simulation	Average Ambient Temperature (°C)	Solar Energy Available (kJ)	Measured Harvested Energy (kJ)	Simulation Harvested Energy (kJ)	Simulated Total Pump Power Used (kJ)
01-Dec-13	2.9	2,084,536	736,337	1,092,300	131,040
08-Dec-13	-15.7	3,555,442	726,862	916,534	93,240
12-Jan-14	2.0	2,397,757	837,623	1,327,100	148,680
15-Dec-13	1.5	5,000,191	1,447,950	1,623,000	138,600
22-Dec-13	-16.2	2,932,361	311,303	737,017	83,160
29-Dec-13	-4.0	3,252,709	1,236,969	1,414,800	176,400

Table 9 summarizes the simulation results for the winter days. The results and examination of simulation output in detail, showed a number of trends that will be explored in more detail throughout this Chapter. During the winter months it was noticed that the system was not performing efficiently, when compared to the summer months and for all instances there was significant heat loss while the fluid traveled between the heat collector and the building interior. It was also noted that during winter conditions, the TRNSYS model was not able to fully imitate the heating system, when compared to the measured values. Similar to summer months, it was noticed that DWH5 was performing below design expectation.

5.5 Efficiency and Utilization Factor

One of the key deliverables of this study is to develop the methodology to assess the feasibility of using similar solar systems in the future. Efficiency needs to be considered so the SLC solar heating system can be compared with other systems. The efficiency of the system is defined as the ratio of the overall energy transferred to the domestic hot water to the sum of the energy available from solar radiation and the energy used by the pump (PI / P2). The coefficient of performance (COP) were also calculated; COP is the ratio of the useful energy output by the system to the energy input.

Table 10: Efficiency from measured and simulated data

Season of Year	Average Ambient Temperature (°C)	Average Solar Energy Available (GJ)	Average Measured Harvested Energy (GJ)	Average Simulation Harvested Energy (GJ)	Efficiency (Measured / Simulated)	COP (Measured / Simulated)
Summer (7 days)	16.1	7.31	3.25	3.13	41% / 43%	14.7 / 14.3
Winter (6 days)	-4.9	3.20	0.88	1.19	27% / 37%	6.7 / 9.3

Table 10 shows the efficiency; for the summer months, the efficiency difference between the measured and simulated values are comparable given the margin of error of all the instruments including the pyranometers. For the winter months, the efficiency differs significantly. The three contributing factors that are suspected to be the cause include:

- the underperforming DHW5 heat exchanger, as explained in section 5.9

- the higher than anticipated heat loss for when the water-glycol mixture travels between the solar collector and the building interior
- the collectors possibly covered by snow or morning frost

When comparing the measured or simulated efficiencies of the system to those by Ayompe and Duffy (2013) in Dublin, 41% in December and 59% in May (Ayompe & Duffy, 2013), it is clear that the SLC efficiencies were lower. As the efficiency variation exists even for the case of the simulated model, the discrepancy cannot be explained by concerns over system maintenance alone (section 5.9). The decision during design of only utilizing the system when heat is needed by the building management system and not having a large heat sink where the thermal energy can be stored is largely responsible. As shown in Table 10; the range of COP was found to be appropriate for the system. A typical COP for an average geothermal system has a COP of approximately 3.3 (Natural Resources Canada, 2016).

Efficiency and COP provide information on the ratio of energy available compared to the energy harvested. Another metric that can be used to evaluate the system is the utilization factor: the ratio of the overall time that the system is operational compared to the total time that the system could be in use. Generally speaking, the utilization factor is used for photovoltaic and wind power system, but not very often for solar heating systems. For the case of SLC, utilization factor is important as the system is not always generating heat when it is available or needed.

Table 11: Utilization Factor from the simulated data

Season of Year	Average Ambient Temperature (°C)	Average Solar Energy Available (GJ)	Average Simulation Harvested Energy (GJ)	Utilization Factor
Summer (7 days)	16.1	7.31	3.13	44%
Winter (6 days)	-4.9	3.20	1.19	27%

Table 11 shows the utilization factor that for the system. As anticipated, the utilization factor was found to be higher during summer months than winter months. Due to a lack of low

temperature load, the heat is not effectively transferred to provide hot water and therefore the efficiency is reduced.

5.6 Economics Analysis

To develop the methodology for assessing the feasibility of similar solar projects, an economic evaluation was conducted. Given the current economic conditions, solar heating systems are not considered to be financially competitive to natural gas heating system. It is important to compare the different options financially to track the performance and the financial outlook for solar heating systems.

Table 12: Average power input and output from the simulated data

Season of Year	Average Ambient Temperature (°C)	Average Solar Energy Available (GJ)	Average Harvested Energy (higher of the measured or simulated values) (GJ)	Electricity Used (MJ)
Summer (7 days)	16.1	7.31	3.25	211.3
Winter (6 days)	-4.9	3.20	1.19	128.5

The energy values used for the economic analysis can be found in Table 12. The summer temperatures could conservatively be considered valid for 8 months of the year. Using the average ambient temperatures recorded, this approach was considered acceptable. The annual energy harvested by the system is estimated to be 938 GJ and the estimated electricity used is 67.2 GJ.

Based on the current natural gas and electricity rates provided for a one year contract ($3.79/GJ and $0.559/kwh respectively), the estimated annual cost of natural gas saved is $3,555 and the estimated cost of electricity consumed to drive the pump is $1,044 (ENMAX, 2015). The transmission and distribution charges saved for the case of the natural gas are estimated to be $179 annually (ATCO Gas Ltd, 2011); for the case of electricity the additional charges are estimated to be $733 (ENMAX POWER CORPORATION, 2017). There is a high discrepancy in the natural gas and electrical charges; the cost saving for the distribution and transmission of natural gas is low because the reduction is during summer months, when the

system is not strained. During the winter months when the system is strained the natural gas savings from the solar system are low (natural gas demand peaks during winter). The electrical connectivity charges are high, as the 5.6 kW power for the pump is the same for both summer and winter months (peak demand for electricity occurs during summer).

The overall estimated savings for commodity and transportation charges for natural gas annually are equal to $3,734 and the additional charges from electricity for the solar system are $1,777. Therefore, system has savings of approximately $1,957 annually. It is important to note that only the cost of electricity and gas was considered; maintenance for either the solar or the natural gas system has not been considered. The natural gas system will always need to be serviced, to maintain a back-up to the solar system. The maintenance cost for the solar system is expected to be much higher than the calculated savings but is ignored as this is a pilot project and costs are expected to decline over time.

The capital cost of the installation of the solar heating system and retrofitting the existing system was approximately $600,000 (Spark, 2011). With the annual savings stated above, the payback period is significant and financially, the solar heat system has no capital advantage over the natural gas system.

The project can also be evaluated using the tons of carbon emissions saved. Assuming efficiency of generating electric of 40%, the annual energy saving is 770 GJ. This is equivalent to overall carbon savings of 52 metric tons annually. Considering the current carbon tax of $20 per ton of carbon emissions, there is an additional estimated annual cost saving of $1,040 from to the solar heating system.

5.7 Maximum Fluid Temperature and Dry Cooler Performance

It was noted previously that there was overheating of water-glycol mixture and fluid temperatures were reaching more than 130°C (Nadeekangani, 2014). These temperatures are extremely high and can cause damage to the system. While reviewing the simulation results for 1 Sept, 2013, as shown in Figure 38, the maximum fluid temperature was higher than 98°C. As

the average temperature goes above 98°C it can be assumed that localized temperatures are higher than the boiling temperature of the water-glycol mixture (107°C).

Table 13: Highest water-glycol mixture temperatures simulated

Date	Average Ambient Temperature (°C)	Average Solar Energy Available (GJ)	Highest Fluid Temperature Simulated (°C)
1 Sept 2013	18.1	11.8	98.29
8 Sept 2013	14.4	9.4	95.74

Table 13 shows the two instances, from the nine summer days that were simulated, when the fluid temperature exceeded 94°C. It is anticipated that there would be a number of other instances over the summer months when the temperature exceeded 94°C and DC-1 is turned on. Due to the high number of instances that DC-1 is anticipated to turn on, it is recommended that the control system be updated to not expel the energy that has already been collected by the system. Once the fluid temperature goes below 75°C, DC-1 should turn off. Currently, this the cut-off temperature is set to 50°C, which is causing the system to exhaust a lot of heat. By turning off DC-1, the energy is stored for a longer duration and can be utilized if there is increased heat demand.

This finding verifies Nadeekangani (2014) claims that the water-glycol mixture is boiling; TRNSYS simulation considers that all equipment is working the way it has been designed. It seems that the set of arrays that were used by Nadeekangani have a lower than anticipated flow. Between the 50 parallel runs of water-glycol mixture, some are expected to have higher flows than others. This could cause some arrays to heat more than average, and thus possibly causing the fluid to boil. Nadeekangani had noticed negative flow and investigated the flow meter. The overheating can cause degradation of the water-glycol mixture. Localized boiling would also cause an increase in pressure and would explain the negative flow recorded by Nadeekangani (2014). This could be prevented by the check valves located on each set of solar arrays. However, if the fluid is in vapor form, it is likely that it can bypass the check valve. It is

recommended that the pump, one-way valves and the flow restrictions for the parallel runs be inspected and replaced as needed, as the flow between all the parallel runs is not the same.

5.8 Investigation of System Improvements

The controller set-up was changed in TRNSYS and the simulation was run to examine how the changes would affect the system performance. There were a number of alternatives that were explored to determine if they would help make the solar system move effective.

5.8.1 Decreasing Temperature Difference Required to Start the Solar System

While observing the system simulation, it was noticed that at times there was energy avalaible in the solar collectors but the system was not turned on. After investiation, it was found that the reason why the solar system was not operational was because the temperature difference between the solar collectors and the DHW5 tank was less than 5.5°C. As per the control system specification, the temperautre difference needs to be greater than 5.5°C for the pumps to turn on. The set temperature difference required for the pump to turn on was reduced from 5.5°C to 2.5°C.

Table 14: Average system outputs when temperature difference required for pump to turn on is reduced

Season	Average Ambient Temperature (°C)	Temperature Difference Required for Pump to on: 5.5°C		Temperature Difference Required for Pump to on: 2.5°C	
		Simulation Harvested Energy (kJ)	Simulated Total Pump Power Used (kJ)	Simulation Harvested Energy (kJ)	Simulated Total Pump Power Used (kJ)
Summer	16.1	3,130,700	211,320	3,078,825	221,130

Table 14 shows the results for summer days with reduced temperature requirements. Winter days were excluded, as for winter conditions, the heat loss was already significant, and increasing the duration of pump operation would only further increase the heat loss (loss would be much higher than the possible heat energy gain). Only in a few cases, was it found that the heat harvested increased due to the change in the settings. Although, additional heat was collected by the panels, more often than not there was a higher heat loss. The reduction of the set temperature difference required for the pump to start reduced the heat delivered to the

domestic water. It was also found that the pump was running for 5% longer which would increase the overall cost of operating the system without any added benefit. It would also reduce the life of the system due to added wear and tear and also additional maintenance cost.

This alternative was not considered to be beneficial and should not be implemented.

5.8.2 Increasing Temperature Difference Required to Start the Solar System

During the testing described in Section 5.8.1, it was realized that the even though decreasing the set temperature difference required between the solar collector temperature and the DHW5 temperature was not beneficial, there was a possibility that increasing the required temperature difference could be beneficial. This could reduce the duration the system is functioning and reduce the energy required for the operation of the system. During the next set of testing, the minimum temperature difference required was changed to get overall better results. From a number of simulations, it was determined that the best results were achieved when the system operated only when an 8°C difference in temperature occurred between the solar collector and the DHW5. This was concluded by reviewing Figure 41, which shows the energy harvested by the system (vertical axis) based on the temperature difference required for the pump to turn on (horizontal axis).

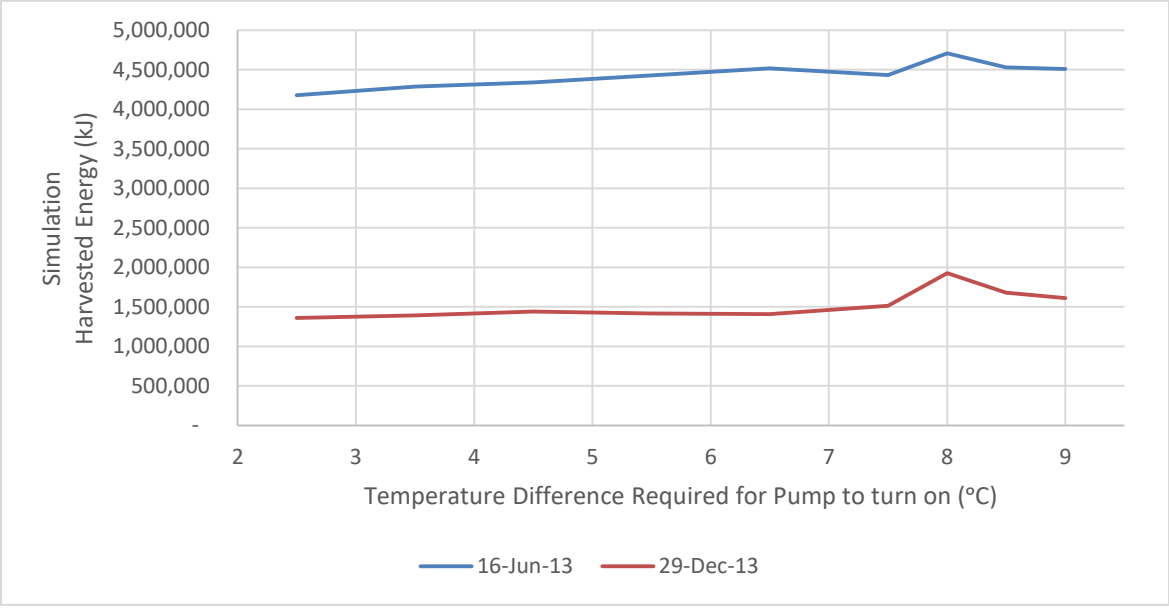

Figure 41: Energy harvested by system based on different set tempererature for pump to turn on

Testing was performed for all days the simulation data was available, to determine the implications of the changes.

Table 15: System outputs when temperature difference required for pump to turn on is increased

Season	Average Ambient Temperature (°C)	Temperature Difference Required for Pump to turn on: 5.5°C		Temperature Difference Required for Pump to turn on: 8°C	
		Simulation Harvested Energy (kJ)	Simulated Total Pump Power Used (kJ)	Simulation Harvested Energy (kJ)	Simulated Total Pump Power Used (kJ)
Summer	16.1	3,130,700	211,320	3,099,900	179,928
Winter	-4.9	1,185,125	128,520	1,441,692	119,280

Testing was performed for all days the simulation data was available, to determine the implications of the changes.

Table 15 shows the results with increased temperature requirements. It was noted that during the winter conditions that the overall system heat output increased by 22%, while the electricity used by the pumps reduced by 7%. It was determined that during the winter conditions the increased temperature difference requirement works well. For the summer conditions, it was noticed that the heat collected on an average day reduced by 30,800 kJ; and the energy consumed by the system reduced by 31,392 kJ. For the summer months, the reduction on the heat collected is not a concern, as the demand is low and the amount of electricity used to collect the additional heat is greater than the heat collected. Due to inefficiencies when producing electricity, this option is preferable.

It was determined that it is advantageous to increase the minimum difference in temperature required between the solar collector and DHW5 for the system to turn ‘on’, to 8°C for both summer and winter months.

5.8.3 Timing of Make-up Water

When running the simulations, it was noticed that the make-up water was often turned ‘on’ at 7 am. It was thought that for certain days, it could be beneficial to have the make-up water

added at 10 am, when the solar radiation is higher than at 7 am. There were five days during the summer months and four days during the winter months for which the simulation was run while delaying the make-up water to 10 am.

Table 16: System outputs when makeup water timing is changed to 10 am

Season	Average Ambient Temperature (°C)	Original make-up water time		10 am make-up water time	
		Simulation Harvested Energy (kJ)	Simulated Total Pump Power Used (kJ)	Simulation Harvested Energy (kJ)	Simulated Total Pump Power Used (kJ)
Summer	14	2,879,360	205,128	3,228,360	198,576
Winter	-6.9	1,092,213	111,510	887,260	105,210

Table 16 shows the results for when the make-up water is delayed. Due to the delay in the make-up water for the summer months, the heat collected by the system increased by 12%, while the energy consumed by the pumps reduced. For the winter months, the energy reduced when the make-up water was delayed; the energy consumed by the pump is also reduced, but not proportionally. The success noticed during the summer months was not observed in the winter months, as the make-up water temperature does not vary dramatically between winter and summer months. During the summer months, the temperature difference between the water-glycol mixture and the make-up water is high and this leads to good heat transfer to the make-up water. This is why it is advantageous to have the make-up water turned ‘on’ when the solar radiation is higher than average. Also, during summer, the energy demand and heat transfer to DHW5 tank is low. For the winter months, the water-glycol mixture is at a much lower temperature when compared to the summer months, but the make-up water temperature has not gone down by the same amount. This causes a lower heat transfer rate and causes the system to not perform as effectively when compared to the summer days.

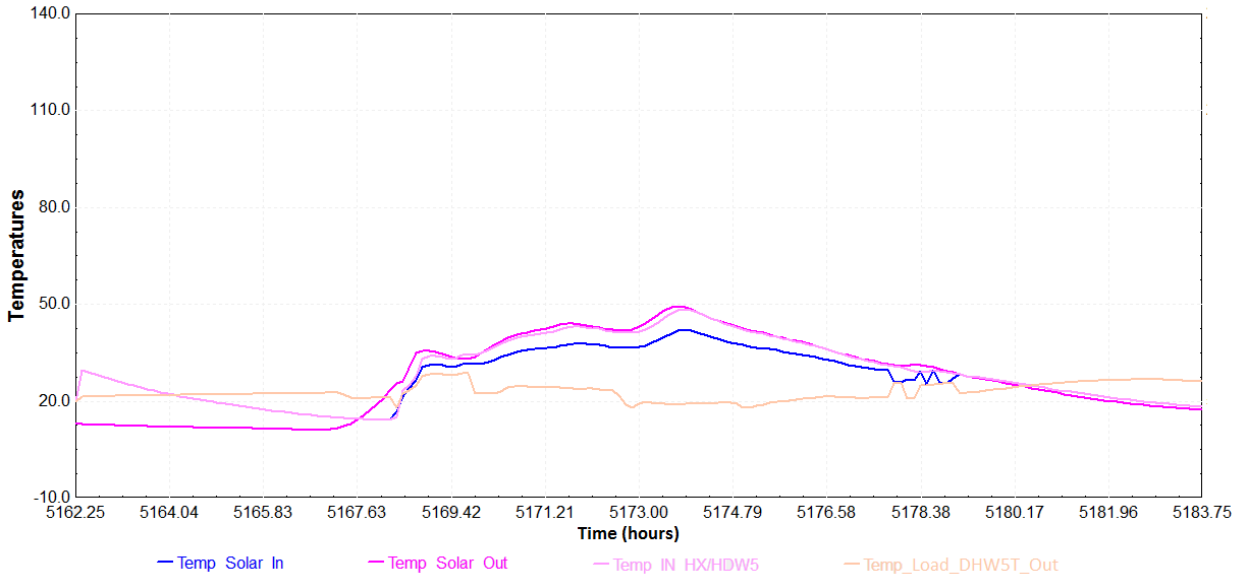

Figure 42: Simulation output graph for 4 August, 2013 with the make-up water time changed (temperature in °C)

Figure 42 shows the simulation output for 4 August, 2013, with the make-up water turning on at 10 am (5,170 hrs). It is recommended that during summer months the operational staff wait until 10 am before they proceed with turning 'on' the make-up water feed. This will help increase the amount of solar radiation that is harvested by the system.

5.8.4 Increasing the Maximum Allowed Temperature of DHW5 Tank

The maximum set temperature for the DHW5 tank to 60°C. For two of the nine summer days that the simulation was run, it was found that the heat demand at the SLC was maximized. After this point, any additional heat harvested from the solar system is not used or stored in the SLC system and has to be exhausted to the environment. One way to increase the heat stored, is to increase the number of tanks where the energy is stored. As an extra tank storage area does not exist at SLC, the easier alternative is to increase the maximum temperature above 60°C. Not being aware of any safety or integrity concerns, it is recommended that the maximum temperature of DHW5 be increased to 80°C.

Attempts were made to simulate the increased set temperature of DHW5 in TRNSYS. There were errors noticed in the simulation, as during the original simulation the array temperatures increased significantly after the pumps turned off and the rate of temperature reduction after

the pump turns back on is significantly lower. For the case of the increased set temperatures for DHW5, the pumps do not turn off. The energy transfer to the water is found to be lower. This is not consistent with expectations and it is assumed that an unexplained simulation error caused this discrepancy.

The DHW5 maximum temperture should be increased and the system performance should be investigated. Figure 43 shows the TYNSYS simulation for 1 September, 2013 after DHW5 set temperature was increased to 80°C. As shown, this should help reduce the incidences when the water-glycol mixture goes over 94°C (compare with Figure 38).

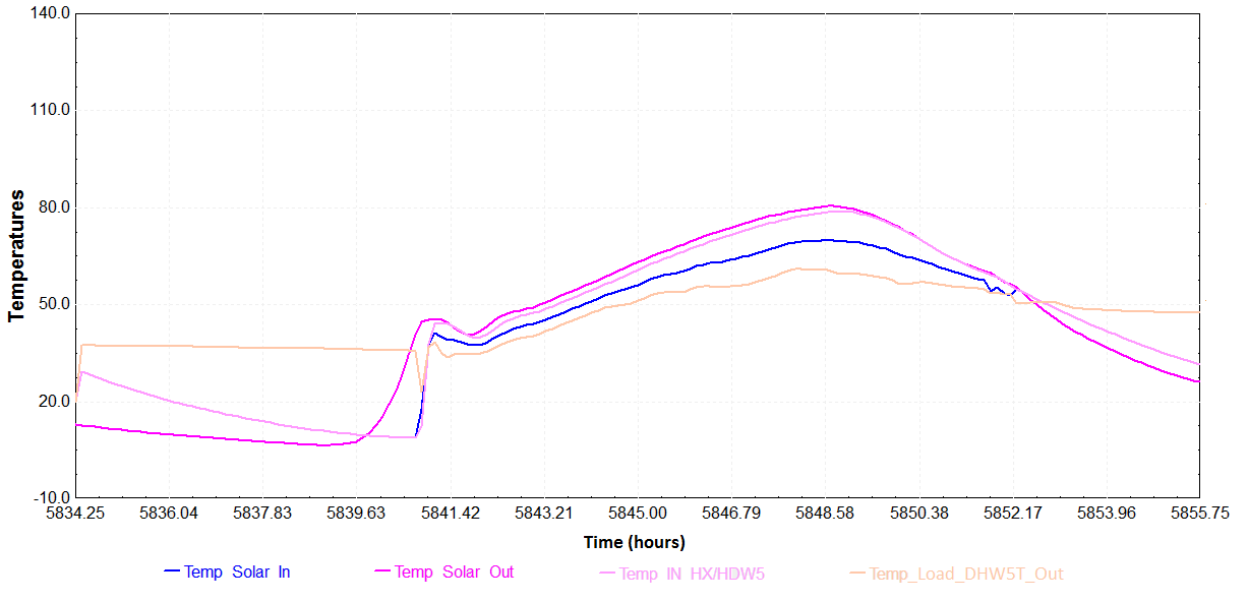

Figure 43: Simulation graph for 1 September, 2013 after DHW5 set temperature was increased (temperature in °C)

5.9 Maintenance Concerns

While exploring alternatives to make the system more efficient, it was noticed that there were operational concerns that needed to be addressed. These concerns were communicated to the operational personnel at SLC.

After it was confirmed from the simulation that the water-glycol mixture temperature exceeded 96°C, it is highly likely that locally the temperatures would be much higher. Although this is not captured by the simulation, which assume ideal operational conditions (same flow in

each of the 50 parallel runs solar runs), this is still of a major concern. Water-glycol mixture temperature, as high as 130°C, was measured in 2014 by Nadeekangani and there has been no changes in operational conditions since. Based on the temperature data recorded, there is risk of localized boiling. As discussed in Section 2.4, the high temperature can make the fluid acidic and deteriorate its properties. When requested, SLC could not provide records for glycol concentration, inhibitor and bacterial testing. The risk with the bacteria is that over time it can biodegrade the glycol mixture, as glycol can act as a nutrient for the bacteria. Testing needs to be performed to check for and control bacteria growth. Inhibitor testing is important, to confirm that the water-glycol mixture is not reacting with the piping and thus causing corrosion loss. Another method to check for inner corrosion is to check metal concentration in the water-glycol mixture; these test records were also not available.

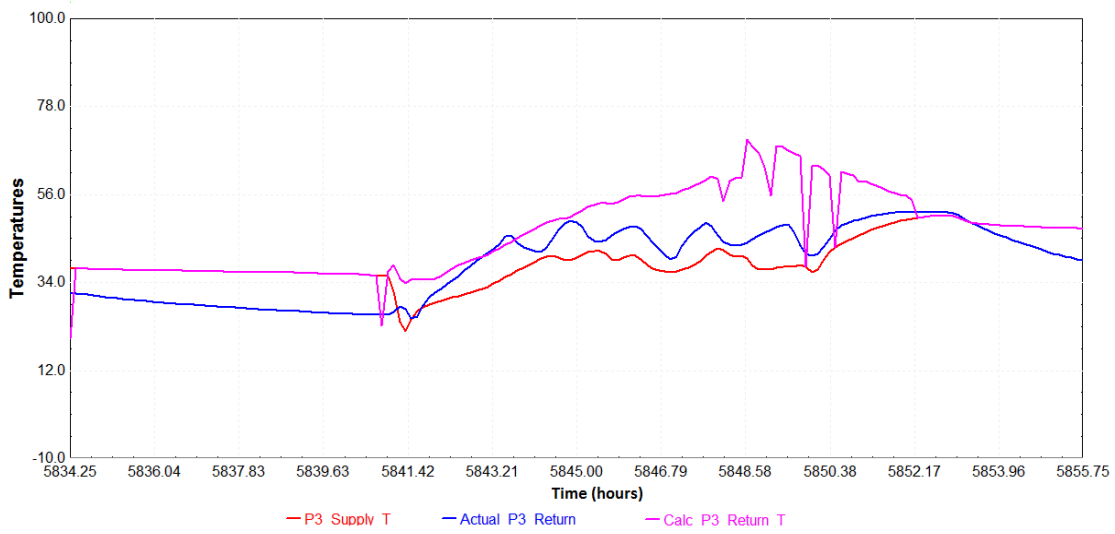

Figure 44: DHW5 inputs and outputs from simulation for 1 Sept, 2013 (temperature in °C)

During the simulation, it was noticed that the DHW5 shell and tube heat exchanger was not able to match its design performance. In Figure 44, 'P3 Supply T' is the fluid outlet temperature at pump P3, 'Actual P3 Return' is the measured fluid outlet temperature from DHW5 and 'Calc P3 Return T' is the simulated fluid outlet temperature from DHW5. The figure shows the output temperature for the actual measured and simulated (calculated) water temperatures for DHW5 for 1 September 2013. It is noted that the actual temperatures are lower than the simulated temperatures which indicated that DHW5 is underperforming the design conditions. The

underperformance can possibly be explained by scaling, loss of fluid properties or over-estimated design conditions from vendor for the DHW5 tank. It is recommended that during a planned outage the tubing be inspected and descaled, if needed.

During the winter conditions, the simulation was outperforming the measured system performance. This can be explained due to shading by snow, wind losses or performance losses due to loss of vacuum in some solar panels. It is recommended that extra effort be placed in ensuring that snow covering the evacuated tubes is removed promptly. It is also worth, at a minimum, inspecting the system annually to check for heat loss sources and failed vacuum seals in the collector tubes. Figure 45 shows the exposed flex piping between the collector manifold and the properly insulated piping; during winter months, the exposed metal piping can cause significant heat loss and should be better insulated.

Figure 45: Solar panels on the roof of Southland Leisure Centre **(City of Calgary, 2012)**

5.10 Considerations for Future Solar Collector Designs and Studies

During the study, it was realized that there are a number of limitations in the system that cannot be resolved due to the original design of the building without a solar heating system.

When considering the heating system, the heat sink, where the energy is stored, needs to be larger. The current system stores the heat in DHW1 and DHW2 tanks. If the heat system was not a retrofit design, the energy could be stored in larger tanks. The system could also be designed in a manner the pool water itself could be used as a heat sink, but this would require a more extensively controlled solar system. If the building was designed to accommodate a solar system, there would not be a need to run piping externally on the roof, as done in the current

model. The pipe could be incorporated in the overall building design and this would dramatically reduce the costs of installation and the heat loss though the outdoor piping.

During the summer months, the system has higher amounts of heat produced when compared to the winter months. As stated by Gill and Goldwater, (2007) the higher performance during summer months makes systems, similar to the solar system at SLC, ideal for outdoor pools in Canada (Gill & Goldwater, 2007). For the current system, the heat has to transfer from the fluid in the evacuated tubed collectors to the water-glycol mixture and then from the water-glycol mixture to the water that is used domestically at SLC. Every change in heat medium adds additional inefficiency to the system. Using the system for outdoor swimming pools would remove the need of using the water-glycol mixture in similar locations like Calgary, as the pool would only be functional during summer months.

The way the system has been setup at SLC, the heat demand is very intermittent, especially during summer months, when the system can perform well. Systems where the heat demand always exists, like process load, should be considered for solar application. Any of these systems could be studied and the system efficiencies can be compared to efficiencies recorded from this study. As stated earlier, wind loss and the resultant affects to the system should also be addressed in future studies.

6 Conclusion and Recommendation

The main goal for this research was to simulate the SLC solar heating system, compute the system performance metrics including efficiency and develop recommendations that would be beneficial for this system and other solar systems. TRNSYS was used to simulate the system, as the available components in the TRNSYS library and its computing power makes it the ideal software for solar thermal energy system similar to the SLC solar system.

The components used in the simulation model were verified before they were used in the completed model. The verification of the solar collector was performed by running the simulation for the solar radiation measured during the collector testing and comparing the simulation performance (Kramer, 2007). The verification was successful in demonstrating that the simulation component was a fair representation of the solar collector used at SLC. The data that was made available for the research was, at times, missing sub-sets that were required for a long time simulation. The pyranometers used had a solar radiation accuracy of 10 percent for the daily radiation and some of the data collected was over the maximum possible values. After the data was filtered to remove the inaccurate data sets, it was found that the data for only 15 of the 363 days collected, could be used in the simulation.

When the actual total natural gas consumed over three years was compared, it was found that the total natural gas consumed was increasing over consecutive years. This could be explained by increased heat demand, operational changes or weather difference between the different years. For the 15 days that the simulation was performed, the solar radiation available to harvest varied between 2.1 GJ and 11.8 GJ. This is a wide range and is caused by variation in weather, including season of the year and local weather conditions. Figure 37 shows the solar radiation observed over the day for a clear sky day and for an overcast day. It was observed that during summer conditions, the simulation was consistently able to mimic the measured system outputs. Certain summer days, when the system heat demand was not high it was observed that DC-1 would turn ‘on’ to assist in ensuring that the water-glycol mixture did not overheat. Nadeekangani (2014) had noted that the working fluid temperatures reached 130 °C. Although, this is how the system is meant to perform, it is not ideal as the energy collected by

the solar collectors ends up being exhausted into the environment instead of being used within the SLC. During winter months, the simulation overestimated the measured values; there were heat loss while the fluid traveled between the heat collector and the building interior. Throughout the year, the DHW5 heat exchanger was underperforming relative to its design and the make-up water was almost consistently being turned on at 7 am. During the extremely cold days the fluid would cool down significantly enough while traveling between the collector and the building during the system start-up that the fluid would end up cooling, instead of heating, the water. For winter conditions, the TRNSYS model was not able to fully imitate the heating system. This was due to the thermal losses and variation of collector efficiency, which is not captured in the model or the efficiency equation.

The measured efficiency for the summer months was approximately 41% and for the winter months it was approximately 27%. These values are smaller than those found by Ayompe and Duffy (2013) in Dublin, 59% in May and 41% in December (Ayompe & Duffy, 2013). The system COP was found to be over 6.7. Due to the high capital cost of the system installation, under the current financial conditions, the solar heat collector system is not financially profitable. If maintenance costs are ignored, the system has savings of approximately $1,957 annually. Not considering the carbon emissions from the manufacturing and installation of the system, the SLC solar system annually saves an equivalent to 52 metric tons of carbon emissions.

Nadeekangani (2014) stated that there could be localized boiling within some of the solar arrays. From the data and the simulation it was verified that Nadeekangani's results were accurate and that not all parallel runs have the same fluid flow rate. It is recommended that the pump flow rate and the flow restrictions be tested and replaced as needed.

There are a number of improvements that can be made to the system. It was confirmed that decreasing the temperature difference required between the solar collector and the load water temperature, for the pump to turn 'on' did not increase the system productivity due to added heat losses through the piping. For winter months, increasing the required temperature difference to 8°C increased the system heat output by 22% while the electricity used by the pumps reduced by 7%. The change was also beneficial during summer months. During the

summer, if the timing of the make-up was changed to no earlier than 10 am, then the heat collected by the system increased by 12%

Based on the finding from the simulation, the list of recommendations includes:

- Future solar systems installed in similar weather conditions should consider using a larger heat sink. Ideally, a heat load that always requires heat should be considered.
- Set the temperature difference required between the solar collector and the load water temperature for the pump to turn 'on' to 8°C.
- Once DC-1 is turned 'on', it should turn off after the water-glycol mixture reaches temperature below 75°C.
- If safety considerations are not involved, the temperature at which DHW5 Tank stops receiving heat should be increased to 80°C.
- Unless necessary, during summer conditions the make-up water should not be turned on before 10 am.
- Inspect, test and replace pumps, one-way valves and flow restrictions as needed.
- Inspect, and if required, descale and test DHW5.
- The water-glycol mixture should be tested for metals, inhibitors, PH and bacterial growth on a routinely bases.
- The collector tubes should at a minimum be inspected annually.
- A detailed TRNSYS or similar simulation be used at the design stage to determine the appropriateness of above recommendations for specific future systems.

Although most of these changes that are recommended have been prompted by the TRNSYS simulation, it is also recommended that that the system data be reviewed after the changes are implemented. Future studies should also try to capture the effects of wind to the performance of the evacuated tube solar collector. Solar heating system should be incorporated for process loads and within the original design of the buildings; the retrofit system was expensive and had lower performance.

References

ATCO Gas Ltd. (2011, December 11). *Current Rates*. Retrieved January 30, 2017, from www.atcogas.com: http://www.atcogas.com/Rates/Current_Rates/

Ayompe, L., & Duffy, A. (2013). Thermal performance analysis of a solar water heating system with heat pipe evacuated tube collector using data from a field trial . *Solar Energy, v 90*, 17-28.

City of Calgary. (2012, July 18). *www.calgary.ca.* Retrieved Feburary 2, 2017, from Green initiatives at Southland: http://www.calgary.ca/CSPS/Recreation/Pages/Leisure-centres/Southland-green-initiatives.aspx

ClenAir. (2013, February 23). *Glycol Percentage Relative to Freeze Point*. Retrieved October 13, 2016, from www.clenair.com: https://www.clenair.com/sites/clenair.com/files/productpdf/Glycol_Values.pdf

Current Results Publishing Ltd. (2011, June 28). *Sunshine in Canadian Cities: Average Hours & Days a Year.* Retrieved June 14, 2016, from Current Results: https://www.currentresults.com/Weather/Canada/Cities/sunshine-annual-average.php

Damaschke, N. (2016, August 15). *Solar Power*. Retrieved September 23, 2016, from Alternative Energy: http://www.tc.umn.edu/~dama0023/solar.html

Department of Energy. (2004, January 3). *https://www1.eere.energy.gov/solar/pdfs/solar_timeline.pdf.* Retrieved September 9, 2016, from US Department of Energy.

Drake Landing Solar Community. (2005, June 18). *Welcome to Drake Landing Solar Community*. Retrieved October 6, 2016, from Drake Landing Solar Community: http://www.dlsc.ca/index.htm

Duffie, J. A., & Beckman, W. A. (2013). *Solar Engineering of Thermal Processes* (4th ed.). Madison: Wiley.

Duffy, M., Bradley, D., & Thornton, J. (2012, October 8). TRNSYS101_Concepts. Madison, Wisconsin, United States.

ENMAX. (2015, July 1). *EasyMax by ENMAX Energy*. Retrieved January 30, 2017, from www.ENMAX.com : https://www.enmax.com/home/electricity-and-natural-gas/easymax

ENMAX POWER CORPORATION. (2017, January 1). *ENMAX POWER CORPORATION ("EPC") DISTRIBUTION TARIFF RATE SCHEDULE.* Retrieved January 30, 2017, from www.enmax.com: https://www.enmax.com/ForYourHomeSite/Documents/2017-01-01-DT-Rate-Schedule.pdf

Fox, K. C. (2016, May 23). *NASA: Solar Storms May Have Been Key to Life on Earth*. Retrieved August 15, 2016, from NASA's Goddard Space Flight Center: https://www.nasa.gov/feature/goddard/2016/nasa-solar-storms-may-have-been-key-to-life-on-earth/

Fred, S. (2010, April 13). *Solar Thermal 101: Flat Plate Solar Collectors*. Retrieved September 27, 2017, from Free Hot Water Solar Thermal Solutions: http://www.freehotwater.com/solar-thermal-101-flat-plate-solar-collectors/

Gill, S., & Goldwater, A. (2007). *OSEA CanSIA Solar Thermal Community Action Manual.* Ottawa: Canadian Solar Industries Association.

Gonzlez, G. R. (2005, August 1). *Solar Energy Potential At Different Latitudes.* Retrieved September 22, 2016, from Altenergymag: http://www.altenergymag.com/content.php?issue_number=05.08.01&article=gonzalez

Gulin, M., Vaˇsak, M., & Baoti´, M. (2013). Estimation of the global solar irradiance on tilted surfaces. *17th International Conference on Electrical Drives and Power Electronics (EDPE 2013)*, (pp. 334-339).

Hathaway, D. (2010, October 21). *Ask an Expert: All About the Sun!* Retrieved August 18, 2016, from NASA Chats: http://www.nasa.gov/connect/chat/solar_chat2.html

Hodge, B. K. (2010). *Alternative Energy Systems and Application.* Starkville: John Wiley & Sons, Inc.

Iqbal, M. (1979). Correlation of average diffuse and beam radiation with hours of bright sunshine. *Solar Energy 23.2*, 169-173.

Islam, M., Fartaj, A., & Ting, D. S. (2004). Current utilization and future prospects of emerging renewable energy applications in Canada. *Renewable & Sustainable Energy Reviews, v 8, n 6*, 493-519.

ITACA. (2005, June 5). *Solar Energy Reaching The Earth's Surface*. Retrieved October 3, 2016, from The Sun As A Source Of Energy: http://www.itacanet.org/the-sun-as-a-source-of-energy/part-2-solar-energy-reaching-the-earths-surface/

Jackman, T., Lonseth, R., Lonseth, A., & Jagoda, K. (2009). Solar thermal water heating: An application for Alberta, Canada. *IASTED International Conference on Environmental Management and Engineering, EME 2009*, 169-174.

Kalogirou, S. A. (2014). *Solar Energy Engineering: Process and Systems.* Oxford: Elsevier Inc.

Kitagawa, K. (2010, Febuary 15). *Putting a Lid on Home Energy Costs.* Retrieved October 8, 2016, from ODEC: http://www.odec.ca/projects/2010/kitaxk2/background.html

Kovacs, P. (2012). *A guide to the standard EN 12975 .* Borås: Technical Research Institute of Sweden .

Kramer, K. (2007). *Test Report: KTB Nr. 2007-07-en.* Freiburg : Fraunhofer-Institute for Solar Energy Systems .

Kumar, D., & Kumar, S. (2015). Year-round performance assessment of a solar parabolic trough collector under climatic condition of Bhiwani, India: A case study. *Energy Conversion and Management, v 106*, 224-234.

Lackner, K. S. (2010). *Comparative Impacts of Fossil Fuels and Alternative Energy Sources.* Royal Society of Chemistry.

Masters, K. (2003, October 1). *How can I find the distance to the Sun on any given day?* Retrieved from Ask a astronomer: http://curious.astro.cornell.edu/our-solar-system/the-earth/41-our-solar-system/the-earth/orbit/80-how-can-i-find-the-distance-to-the-sun-on-any-given-day-advanced

McIntire, W. (1982). Factored approximations for biaxial incidence angle modifier. *Solar Energy, 24 (4)*, 315.

Monto, M., & Pillai, R. (2010). Impact of dust on solar photovoltaic (PV) performance: Research status, challenges and recommendations. *Renewable and Sustainable Energy Reviews 14, no. 9*, 3124-3131.

Nadeekangani, A. D. (2014, September). Performance of the Solar Thermal Hot Water System at the Southland Leisure Centre . Calgary, Alberta, Canada: University of Calgary.

Natural Resources Canada. (2016, June 29). *Heat Pumps*. Retrieved Feburary 19, 2017, from http://www.nrcan.gc.ca: http://www.nrcan.gc.ca/energy/publications/efficiency/heating-heat-pump/6831

NREL. (2017, Feburary 7). *Best Research-Cell efficiencies*. Retrieved Feburary 13, 2017, from National Renewable Energy Laboratory: http://www.nrel.gov/pv/assets/images/efficiency-chart.png

Quaschning, V. (2004). Solar thermal water heating. *Renewable Energy World*, 95-99.

Sandry, J. (2013, August 27). *5 Reasons Solar is Already Beating Fossil Fuels.* Retrieved from Solar Moaic: https://joinmosaic.com/blog/5-reasons-solar-already-beating-fossil-fuels/

Solar Pannels Plus. (2008, Jan 4). *Evacuated Tube Solar Water Heating Collectors*. Retrieved October 1, 2016, from Solar Pannels Plus: http://www.solarpanelsplus.com/evacuated-tube-collectors/

Spark, R. (2011, June 9). Supervisor, Facility Operations, Southland Leisure Centre. *Southland Leisure Centre goes Solar Thermal*. (C. o. Calgary, Interviewer) Calgary: City of Calgary. Retrieved January 15, 2017, from https://www.youtube.com/watch?v=ojkPsWKNXH8

Taube, H., & Carscallen, W. E. (1985). Three year operating experience with a 281 M2 ETC Solar Energy Facility in Edmonton, Alberta, Canada. *Intersol Eighty Five: Proceedings of the Ninth Biennial Congress of the International Solar Energy Society*, 988 - 992.

Thermal Energy System Specialists. (2011, June 19). *What is TRNSYS?* Retrieved November 28, 2016, from TRNSYS: http://www.trnsys.com/

Thermal Energy System Specialists. (2012, March). Component Libraries for the TRNSYS Simulation Environment. *Solar Library Mathematical Reference, 10*. Madison, Wisconsin, USA.

Thermal Energy Systems Specialists. (2012, March 12). TESSLibs 17 Volume 06 HVAC Library Mathematical Reference. Madison, Wisconsin, USA.

Thermal Energy Systems Specialists. (2014, May 8). TRNSYS 17 Volume 4 Mathematical Reference . Madison, Wisconsin, U.S.A.

Theunissen, P., & Beckman, W. (1985). Solar transmittance characteristics of evacuated tubular collectors with diffuse back reflectors. *Solar Energy, 35 (4)*, 311-320.

U.S. Energy Information Administration. (2015, March). *Monthly Energy Review, Table 1.3 and 10.1, Preliminary Data*. Retrieved September 15, 2016, from Energy Information Administration: http://www.eia.gov/energy_in_brief/article/major_energy_sources_and_users.cfm

Zhao, H.-z., Liu, Z.-y., Zhang, M., Huang, C., Wang, L.-h., & Zou, Z.-j. (2009). A mechanical and experimental study on the heat loss of solar evacuated tube. *Journal of Shanghai Jiaotong University (Science), Volume 14, Issue 1*, 52–57.